Seeking for Optimal Excited States in Photoinduced Electron-Transfer Processes The Case Study of Brooker's Merocyanine

Yann Danten, Carlo Gatti, Christine Frayret

Seeking for optimal excited states in photoinduced electron-transfer processes – the case study of Brooker's merocyanine

Yann Danten,[†] Carlo Gatti[‡] and Christine Frayret *[,§]

† Institut des Sciences Moléculaires, UMR CNRS 5255, Université de Bordeaux, 351 Cours de la Libération, 33405 Talence, France

‡CNR SCITEC, CNR Istituto di Scienze e Tecnologie Chimiche ''Giulio Natta'', Sede Via C. Golgi, 19, 20133 Milano, Italy

§ Laboratoire de Réactivité et Chimie des Solides (LRCS), UMR CNRS 7314, Université de Picardie Jules Verne, Hub de l'Energie, 15, Rue Baudelocque, 80000 Amiens Cedex, France. Réseau sur le Stockage Electrochimique de l'Energie (RS2E), FR CNRS 3459, France.

ABSTRACT

Material design enters an era in which control of electrons in atoms, molecules and materials is an essential property to be predicted and thoroughly understood in view of discovering new compounds with properties optimized toward specific optical/optoelectronic applications. π-electronic delocalization and charge separation/recombination enter notably into the set of features that are highly desirable to tailor. Diverse domains are particularly relying on photoinduced electron-transfer (PET), including fields of paramount importance such as energy production through light-harvesting, efficient chemoreceptive sensors or organic field-effect transistors. In view of completing the arsenal of strategies in this area, we selected as case study the Brooker's merocyanine – a typical [D-π-A] compound – and examined from Time Dependent Density Functional Theory (TD-DFT) the opportunity offered by selected excited states to reach a suited manipulation of the charge transfer (CT) extent. In addition to the consideration of diagnostic tools able to spot the charge amount (*i.e.* magnitude of electron fraction) transferred upon excitation (q_{CT}), the spatial extent associated with such electronic transition or charge transfer length (D_{CT}) as well as the corresponding variation in dipole moment between the ground and the excited states ($|\boldsymbol{\mu}_{CT}|$), further analysis of the excitation process was undertaken. The advantage of going beyond the above-mentioned molecular indicators – which can be considered as Photoinduced electron-transfer (PET) global indices – was explored on the basis of a partitioning of the electron density. Relevant insight was gained on the relation these global indices have with the evolution of (local) features characterizing either chemical bond or electron delocalization upon vertical excitations.

KEYWORDS: D−π−A push-pull systems, Vertical excitations, Photoinduced electron-transfer, Intramolecular charge transfer (ICT), Electron density partitioning, Quantum Theory of Atoms in Molecules (QTAIM), Charge Transfer (CT) and delocalization indices, Structure − property relationships, Solvatochromism

INTRODUCTION

Photoinduced electron-transfer (PET) also known under other labels such as photoinduced intramolecular charge transfer (P-ICT), or simply intramolecular charge transfer (ICT) is at the heart of various chemical, physical or biological processes in link with widely investigated applications areas. The latter notably include light-to-chemical energy conversion, molecular photoelectronics, photocatalysis or photosynthesis. The ability to tune or improve charge transfer (CT) and the subsequent effect of charge separation (CS) is pivotal to the advances of a large set of research fields. Therefore, identifying key factors involved in the mechanism of ICT constitutes the prerequisite for designing optimized systems. PET is notably occurring in electron donor (D)−electron acceptor (*i.e.* electron withdrawing group) (A) molecules or in systems involving a bridge in between these two moieties, *i.e.* donor−bridge−acceptor [D−B−A] also labelled donor−π−acceptor [D−π−A] compounds. In such systems, the bridge corresponds to a conjugation entity covalently connected to both (D) and (A) and therefore constitutes a support for the electron transport between them. Upon energy absorption, the initial GS in principle leads to a formal $[D^{+}-\pi-A^{-}]^{*}$ excited state. A departure of such a simplified model may however be observed in real cases, the fine details of the electron transfer process being in fact affected for instance by the nature of donor and acceptor subunits and their spacing (*i.e.* bridge type/length). Furthermore, the behavior of these molecular moieties is also influenced by extrinsic parameters, like the surrounding solvent medium polarity or the possible specific interactions that may occur with the solvent molecules. Both aspects are intimately mapped into the evolution of the electronic density upon excitation and most often lead to a situation which is far from that of the ideal one-electron transfer [1-3], such a departure clearly depending notably on geometric and electronic coupling features.

For such push-pull systems, it is crucial to quantify both the length and the magnitude of CT owing to the fact that excited states (ESs) with highly efficient charge separation features are required to reach targeted properties such as the ultrafast interfacial electron injection [4] and because, as stated above, real systems do not obligatory transfer exactly one electron from the donor towards the acceptor. The photo-excitation – PET intimate link is notably of seminal relevance in the field of dyes used in the dye-sensitized solar cells (DSSCs) devices. In this context, accurate examination and identification of the various ESs of chromophores that would be propitious (*i.e.* charge

completely separated states) can be undertaken for instance by focusing on the dye/TiO_2 complexes involved through aggregation effects and by exploiting the estimation of charge density difference of a series of successive excited levels, with respect to the ground state (GS) of such entities. [5] Owing to the fulfilment of many structure-property requirements for use as dye in DSSCs, cyanines – consisting in two nitrogen centers located within heterocycles and separated by a polymethine bridge – constitute a well-studied class of push-pull systems. Likewise, merocyanines (or donor–acceptor substituted neutral polymethines) enclose two terminal heteroatoms (generally a Nitrogen atom and an Oxygen from a carbonyl group) along with a polymethine chain. In this research area as well as in other application fields, engineering new performant push-pull compounds most often relies on a screening for optimal D/A entities and bridge kinds/lengths (along with their most suited combination) or even on proposing new architectures. For instance, it has been observed that systems separating the acceptor group from the anchoring one through the inclusion of an extra π-conjugation unit, (*i.e.* [D−π−A−π−anchor motif]) leads to over 6.5 times higher power conversion efficiencies compared to the conventional [D−π−A] dye [6]. Beyond their interest in the sector of DSSCs research, D–π–A systems and more generally CT dyes, find applications in a very broad context. Besides their direct applicability as solvent polarity probes [7], they were considered notably for photo- (PL) and electro-luminescent (EL) materials in dye lasers [8,9], sensors [10], light-emitting cells (LECs) [11] or optical light emitting diodes (OLEDs) [12] and have also been developed for conceiving many advanced functional materials/devices. For all these purposes, the development of diagnostic indices, enabling to finely spot the metrics for molecular electronic excitations, is essential to systematically screen for new optimal materials. Additionally, apart from the overall search for push-pull systems with prominent PET at the lowest lying singlet excited state, studying further involved ESs beyond the bright $S_1 \leftarrow S_0$ transition of push-pull systems may be of relevance for certain applications. This is especially the case for the differentiation between cyanine, (CT) or mixed cyanine-CT character for the development of two-photon absorption (2PA) and optical power limiter compounds (OPL) applications in the Near Infrared (NIR) spectral range. [13]. Moreover, the recent achievements in the field of attochemistry will surely provide new ways of manipulating electron distributions in electronically ESs. In link with very short duration, the attosecond pulses are characterized by a large spectral bandwidth potentially able to generate several states which are populated in a coherent manner, thus corresponding to an electronic wavepacket. This new field will certainly lead to new opportunities and challenges compared to conventional photochemistry [14].

In this investigation, a reference [D−π−A] compound belonging to the cyanines family – the 1-methyl-4-[(4-oxocyclohexadienylidene)ethylidene]-1,4-dihydropyridine – also called the Brooker's Merocyanine (BM) [15] – was selected in view of offering a unique opportunity to thoroughly examine both the photoinduced charge separation of the vertical excitation transition $S_1 \leftarrow S_0$ and that

occurring in few other low-lying singlet ESs, S_n, with n = 2, 3, 4. In the case of the BM molecule, the electron donor, D (CH_3N) and the electron acceptor, A (CO) groups are separated by aromatic chains and double conjugated bonds, which enable the electron drift between these two components. BM is well-known for its fine tuning of chemical bonding features accompanying electronic CT across the molecule. The notion of CT occurring under photo-excitation in this system is the ability of the molecule to switch its electronic structure from a quinonoid pro-aromatic $(BM)_q$ structure to an aromatic benzenoid $(BM)_b$ one or reversely. Indeed, interpretations of BM electronic spectra features usually rely on the assumption that its electronic structure can be described as a *resonance hybrid* between two *contributing structures:* a *non-charge-separated one (*covalent, strongly bond-alternated, neutral polyene-like, *i.e.* $(BM)_q$*)* and a *charge-separated one* (bond-alternated, zwitterionic form, *i.e.* $(BM)_b$) (Figure 1, see *e.g.* [16]). These structures are sometimes labelled alternatively N ("non-charge-separated contributing structure") and S ("charge-separated contributing structure") or "uncharged contributing structure"/"dipolar contributing structure", respectively, as initially proposed by Leslie G.S. Brooker [17].

In PET phenomena, the transition linked to photonic uptake by the solute is responsible for a charge transfer absorption band, this mechanism being related to a variation in dipole moment from the GS to the ES. Intramolecular charge transfer (ICT) absorption bands are therefore both strongly solvent dependent and indicative of π-electronic transfer between end groups. The most common situation corresponds to the previously mentioned final $[D^+-\pi-A^-]^*$ ES, through a donor to acceptor CT phenomenon, resulting from the transition between the GS (S_0) and the first singlet ES (S_1). This process can be labelled more precisely a forwards CT or "light"-induced increase of the dipole moment characterizing "positively" solvatochromic dyes. It is thus associated to a bathochromic (or positive) shift of the maximum absorption wavelength λ_{max} (CT) (and thus to a band transition energy augmentation) for rising polarity media. While the generic ICT term usually presupposes such kind of situation, reversely, the less common case for which the charge flow takes place from an acceptor to a donor group is another kind of CT effect. It occurs for "negatively" solvatochromic dyes. It thus corresponds to a backwards CT or to a "light"-induced dipole moment decrease, *i.e.* a reduced dipole moment in the excited state (see *e.g.* [18-20]). In that case, where charge transports back from A to D upon photoexcitation ($[D^--\pi-A^+]^*$ excited state) in contrast to what happens for the traditional positive solvatochromic dyes, the solvatochromism phenomenon exhibits an hypsochromic (or negative) shift with increasing solvent polarity (*i.e.* decrease of band transition energy). Alternatively, dyes may belong to a third class of compounds labelled "inverted", or "reverse", if they are characterized by both positive and negative solvatochromic behavior, in a sufficiently wide range of solvent polarities. These dyes may thus be characterized by a bathochromic (or positive) shift effect (also called red-shifted effect) in non-polar solvents, and then hypsochromic or (negative) shift, *i.e.* blue-shifted effect in rising polar media. Owing to the interest of reverse solvatochromic anionic probes [21-23] and due to the propension of

'solvatochromic switches' to exhibit remarkable optical changes in response to subtle modifications in solvation microenvironments – therefore being useful in the design of smart materials – a growing interest currently arises for this kind of compounds. Despite some lack of firm experimental confirmation owing to the low solubility of BM in low polarity media, the solvatochromism of BM – which was formerly identified as being of negative type in polar solvents – is presumably of such reverse type, various studies having provided some clues towards this conclusion. [24-29] By considering that it belongs to this kind of solvatochromic compounds, BM is therefore supposed to exhibit a bathochromic and then a hypsochromic shift of the long wavelength π-π* absorption band as the solvent polarity increases. Concerning the BM structure at the GS, the benzenoid (or charge separated) form should dominate in polar solvents, whereas the quinonoid (or neutral) form should be favoured in non-polar solvents. Nevertheless, such two-state model simply based on neutral/zwitterionic forms is most often considered as being insufficient to adequately describe the absorption spectra. Additionally, a so-called "cyanine-like limit", (CL) (or simply "cyanine limit") [30,31] or "polymethine-like" [32,33] $(BM)_{pm}$ (non-alternated, Figure 1) state being in between the quinonoid and benzenoid extrema is thus usually taken into account. In this particular form, it is supposed that the two above-mentioned contributing structures contribute equally (*i.e.* equal mixture of these two degenerate limiting mesomeric forms), this statement being done by assuming that the equilibrium geometry in the GS S_0 [$R_e(S_0)$] and in the first excited electronic state S_1 [$R_e(S_1)$] are equal.

With the hope of fully rationalizing or eventually predicting the solvatochromic behavior, the quest for an accurate quantification of the relative contribution of the two initially proposed limiting (N or S) forms to the equilibrium structure of the GS in various solvation media has always attracted a great interest and has led to several approaches. Initiated by Förster [34] and later by Platt [35], a simple valence bond (VB) model was developed, aimed at estimating the π-charge distribution in the donor–acceptor-substituted polymethines according to a simple two-state model. In this latter, the contribution of the two resonance structures is considered to strongly depend on the strength of the electron-donor and electron-acceptor groups, *i.e.* "donor−acceptor strength", corresponding to the energy difference between N and S VB-structures. It relies on the assumption that the Eigenfunctions of the electronic GS $\psi(S_0)$ and first electronic ES $\psi(S_1)$ can be approximated as a linear combination of the wavefunctions of the two contributing structures ψ_N and ψ_S and involves solving the corresponding 2 × 2 secular determinant. Such formalism is also referred as "cyanine limit" model. It notably enables to determine the c value, corresponding to the mixing coefficient, the $\psi(S_0)$ and $\psi(S_1)$ relative weights being dependent upon the square of this coefficient, c^2. At the CL, when using this model – c^2 being equal to 0.5 – an equivalent contribution of the valence bond wave functions ψ_N and ψ_S to both S_0 and S_1 is involved. Alternatively, it was then demonstrated that c^2 can also be accessible through an electrooptical approach, which is able to estimate dipole moments and their changes on excitation in a given solvent. [36] Within such

approaches, structures with charges on different atoms representative of another potential kind of electron flow are not taken into account, whereas they should nevertheless also mix to the total wave function. They are omitted and thus neglected in this context. Owing to the difficulty to account for the alternating π-charge densities along the polymethine chain of merocyanine dyes, which were observed from the chemical shifts in ^{13}C nuclear magnetic resonance (NMR) spectrum, intermediate charge-transfer states have therefore been called to account for the interpretation of the spectroscopic properties of these compounds [37-38]. Accordingly, the limitation of the CL model has already been outlined by demonstrating that the electronic structure of some merocyanines cannot be adequately depicted through a linear combination of the two limiting forms N and S. Instead, it was proposed that the alternating π -charge densities in the chain have to be described only by taking into account all limiting forms with a positively charged carbon atom in the polymethine chain [38]. Otherwise, concepts of chemical bond analysis (especially the bond-length alternation (BLA), – defined to be positive for the neutral form while it takes negative values for the charge-separated one – and the closely related average π-bond order alternation (BOA) [39]) are ubiquitous in this field and constitute a route towards the discovery of clues able to quantify the contribution of the two limiting forms to the equilibrium structure of the GS. By considering that negative charge is transferred from the less to the more electrophilic fragment of the dye during the PET process and that such flow is modulated by the nature of the solvent, a general framework in view of rationalizing the solvatochromic behavior of pyridinium phenolate betaine dyes (including BM) was also extracted later from the estimation of variations with the medium of the electrophilic Fukui functions of their electron-pair donor and acceptor moieties. [40] According to this model, all solvatochromic plots of solubilized dye transition energies *vs.* solvent polarity are characterized by a minimum, which can either occur within the experimentally available range of solvent polarities, thus characterizing a “true” reversal or which can alternatively fall beyond this range. In this latter case, the situation leads to a “virtual” or “imaginary” reversal, beyond the range of experimentally available solvent polarities, and thus corresponds either to a positive or negative solvatochromic dye. This formalism was found in agreement [41] with the recent application of the cyanine limit model. [42] Apart from the indications about possible models that can eventually be employed, it shall be outlined that specific solute-solvent interactions shall be taken into account while this aspect was not systematically considered within these various approaches. Indeed, it is recognized that spectral behavior relative to solute electronic transitions are also dependent upon this effect, a recent experimental study having even demonstrated that : i) negative solvatochromic dyes exhibit a strong response to hydrogen-bond (HB) donor solvent acidity (SA) and, on average, a two times lower response to solvent dipolarity (SdP) ; ii) positive solvatochromic dyes also respond to the same solvent properties as negative ones but in a less intense manner, adding a notable sensitivity to the solvent polarizability (SP). [43]

In this context of ICT and solvatochromism features analysis for push-pull [D−π−A] systems, which are of high general interest for many applications and for which some long-standing questions are – as a whole – still pending, a thorough quantum chemical route is employed in this study. It notably relies on a combined estimation of PET global indices [44] along with their atomic group decomposition [45] and the consideration of chemical bonding/electron delocalization evolution, gained through an accurate analysis of electronic structure following TD-DFT calculations. Applied to the dissolved *trans*-BM compound (selected here as a representative probe), the purpose of this investigation is to achieve a detailed microscopic understanding of the electronic structure modulation induced by the absorption transitions relative to singlet ESs. The intercrossed effects of both i) nature of solvation kind (the solvents ranging from polar - supposed to be fully or highly dissociative - to apolar, *i.e.* likely to be much less or almost not dissociative ones and involving as well protic/aprotic kinds, and thus the occurrence of solute-solvent HB interactions for the former type) and ii) switching from the $S_1 \leftarrow S_0$ transition to the one based on a few further low-lying ESs (*i.e.* $S_n \leftarrow S_0$). Rather than being aimed at thoroughly studying in detail the solvatochromism of BM, this investigation is intended to examine the aptitudes of the selected approach to eventually enlighten several microscopic aspects, which are of relevance in the broad area of ICT observed in push-pull systems. After a presentation of GS/ES dipole moments and correlative ICT features for the whole set of solvation conditions/states considered here, we therefore propose – thanks to representative examples – to focus on a potentially more precise level of information gained concerning ICT peculiarities, enclosing: i) the role of solvent modulation on ICT ii) the strongly localized/delocalized ICT situations iii) what brings to excitations with very high ICT features iv) a focus on situations leading to Forward-ICT.

COMPUTATIONAL DETAILS

In the present work, the ground- and excited-state characteristics of *trans*-BM gained through DFT and TD-DFT, enabled to give an overview of the vertical excitation energies (E), absorption peaks (*i.e.* maximal absorption wavelengths, λ_{abs}) and oscillator strengths (*f*) for the $S_n^{FC} \leftarrow S_0$, where FC stands for Franck–Condon, hereafter simply labelled: $S_n \leftarrow S_0$ (with n = 1, 2, 3, 4) absorption transitions (Table SI-1) within a large set of solvation media. These quantum chemical calculations have been carried out using Density Functional Theory (DFT) and Time-Dependent DFT (TD-DFT) procedures implemented in the Gaussian 16 software package [46]. Geometry optimization (S_0 or singlet ground state (GS)) and TD-DFT treatment for the vertical ESs (S_1, S_2, S_3, S_4 considered with the GS geometry) were all performed using the long range corrected (LRC) Coulomb attenuated B3LYP *xc* functional CAM-B3LYP [47] with the cc-pVDZ basis set and by systematically

including solvent effects through implicit SMD solvation model [48]. The selected *xc* functional presents the cumulated advantage of having been recognized as one of the best ones to yield an accurate description of ground-state geometries as well as electronic and geometrical characteristics of excited states, both in gas-phase and in solution, for organic chromophores [49-51] and of being among the most suited functionals to calculate the global CT indices like $|\boldsymbol{\mu}_{CT}|$ (defined hereafter) [52]. It is characterized furthermore by an average error which is independent of the degree of CT in the excitations [53, 54]. It is generally in very good agreement with coupled-cluster results – at least for neutral chromophores – in terms of oscillator strengths and excitation energies [55, 56].

Beyond their recognized implication in solvatochromism features, the formation of hydrogen bonds (HBs) between the carbonyl end of the BM molecule and the hydrogen atom of water solvent molecules has been suggested, even in the crystallized form of BM including structural solvent molecules [57,58], therefore highlighting the need to consider explicit solvent molecules around BM in any circumstance. The strategy of including either one or two explicit solvent molecules through an H-bonded complex involving the carbonyl group of BM has thus been adopted in this work, in the case of polar protic solvents especially (the whole set of concerned cases being indicated on Figures). Whenever the possibility of occurrence of HBs with the carbonyl end of the BM molecule has been probed, explicit solvent molecules were thus placed in the neighborhood of the C=O entity (and relaxed during the geometry optimization), in addition to the concomitant consideration of implicit dielectric effect of solvent through SMD. These situations involving either one or two explicit solvent molecules are labelled: BM+ES_1 and BM+ES_2 systems, for one and two explicit solvent molecules respectively. In this kind of solvent media, the case of BM+ES_2 situation involving two explicit HBs being supposed to be more representative of the real one, it has been selected among these two possibilities for the forthcoming interpretation of results (and for the representation of Figures 2 and 3) while the complete set of data is gathered in the various Tables from SI; *i.e.* in Table SI-1: Vertical excitation energies, wavelengths and oscillator strengths for $S_n \leftarrow S_0$ transitions and Table SI-2: Dipole moment, $|\mu|$ in vertical ESs $S_n \leftarrow S_0$). Table SI-3 indicates the various CT indices for the $S_n \leftarrow S_0$ transitions in all implicit solvation situations. Otherwise, structural features related to solvation of BM + ES_1 and BM + ES_2 systems for the relaxed GS geometries including explicit solvents in the neighborhood of BM are presented on Figure SI-1.

First the DFT-optimized geometries were obtained using a tight criterion of convergence. The local energy minimum nature of these structures gained in S_0 was confirmed from the (harmonic) vibrational analysis (no imaginary frequency). In a second step, the electronic properties were evaluated in the fourth first ESs from the structures obtained in GS using the TD-DFT-procedure. Within this latter approach, the relaxation of the electron density, obtained by applying the Z-vector post-linear response approach, [59] was demonstrated to improve notably the

reliability of the excited state properties, including the density-based indices [60] The wavefunctions obtained through DFT and TD-DFT computations (Gaussian .wfn files) were analyzed in the context of Quantum Theory of Atoms in Molecules (QTAIM) [61] by suitably modified versions of the Bader's PROMEGA program [62]. Studies and analysis of the ESs properties along with their changes relative to the GS calling to (QTAIM)-based or (QTAIM)-related approaches have been previously published (see ***e.g.*** the few recent representative examples given in Refs. [63-72]. Additionally, the present investigation makes use of a new procedure (code labelled DOCTRINE) [45] that, besides evaluating the PET global indexes[44] with greatly enhanced accuracy, allows for decomposing their values into group contributions. This last aspect offers an opportunity to focus on more local CT features gained on the various pieces of the molecule. The results originating from such decomposition (though limited in the present paper to the difference within a molecular group between the local increments and the local depletions of electronic charge upon excitation) along with electron delocalization features were considered as a complement of the following estimated PET global indices [44]: i) the transferred charge, $|q_{CT}|$, ii) the charge-transfer length representing the distance over which CT has occurred, noted (D_{CT}), (*i.e.* the distance between the two CT barycenters), and iii) the transition dipole moment, $|\boldsymbol{\mu}_{CT}|$. It is estimated through the following equation: $|\boldsymbol{\mu}_{CT}| = |\boldsymbol{\mu}_{ES} - \boldsymbol{\mu}_{GS}| = D_{CT} \cdot q_{CT}$, thus corresponding to the variation of the dipole moment between excited state and the GS, in link with the vertical excitation process, where $|q_{CT}|$ is the transferred charge during the $S_n \leftarrow S_0$ transition and D_{CT} is the distance between the two CT barycentres resulting from ICT accompanying the excitation process. $|\boldsymbol{\mu}_{CT}| = D_{CT} \cdot \int \rho^+(\mathbf{r}) d\mathbf{r}$ (which must be equal to $D_{CT} \cdot \int \rho^-(\mathbf{r}) d\mathbf{r}$) and where $\rho^+(\mathbf{r})$ and $\rho^-(\mathbf{r})$ represent, respectively, the local electron density increase or decrease upon vertical excitation). Both $\rho^+(\mathbf{r})$ and $\rho^-(\mathbf{r})$ are taken as definite positive quantities in the integrals above with $\int \rho^+(\mathbf{r}) d\mathbf{r}) \equiv \int \rho^-(\mathbf{r}) d\mathbf{r}$ being equal to the transferred charge, q_{CT}. For the BM+ES_1 and BM+ES_2 systems, the adopted wavefunction (.wfn) files were those related to restraining excitations and charge transfer to the BM molecule (*i.e.* wavefunction generated by setting zero charge on solvent molecules using the basis set of the complete system). Using these specific .wfn files, we have verified that no CT occurs to the explicit solvent molecules, even when QTAIM space partitioning is adopted. The QTAIM net charge on all explicit solvent molecules has been always found to be below $\pm 5 \cdot 10^{-3}$ electrons for all investigated cases.

RESULTS and DISCUSSION

The section presenting the various gathered results and their interpretations is organized as follows. In part 1, the dipole moments were first collected for both the singlet GS, (S_0), and the low-

lying ESs: S_1, S_2, S_3 and S_4. The modulation of the PET involved in the various transitions and according to the nature of the solvent type were then thoroughly examined. CT extent was first characterized by various indicators (part 2), deriving from the variation of the overall electron density of the molecule during an excitation. Such quantification of PET extent was assessed through the estimation of (D_{CT}) and ($|\boldsymbol{\mu}_{CT}|$) in link with the transition $S_n \leftarrow S_0$ which is involved. Furthermore, knowing the location of the displaced positive and negative charge barycenters may be useful to discriminate between the "locally excited" (LE) states and the "charge transfer" (CT) excited states. In the former the electronic perturbation is localized in only one portion of the molecule, while the latter correspond to real exciton states [73,74]. To enhance the degree of knowledge for the ICT phenomenon, additional information on its nature is provided – for a few selected cases - by relating the PET global indices to the evolution – upon vertical excitation – of the (local) features characterizing either chemical bonding or electron delocalization in the BM molecule (part 3.1 to part 3.4). In order to translate the observed trends of the PET global indices into even more easily graspable chemical changes, a focus on results gained through the atomic group decomposition of the charge transferred upon excitation is reported in part 4. To facilitate the results interpretation, the series of investigated solvents presented in the Tables SI-1, SI-2, SI-3 and Figures 2, 3 are arranged in direction from weak polar non-hydroxyl solvents to strong polar protic ones.

1. GS/Excited-state dipole moments

An insight concerning the various excited-state dipole moments (μ) is presented in Figure 2 (also indicated as a whole in Table SI-2) in view of providing a first indication on the extent of charge separation occurring in the GS or for each of the corresponding short-lived ESs. The charge redistribution occurring as a consequence of the passage from GS (*i.e.* S_0) to a certain excited state – related to PET extent – will be explicitly presented hereafter. Figure 2 exhibits a clear trend of modulation of μ as a function of the excited-state kind (1, 2, 3 or 4), involving not only a differentiation with respect to S_0 values but also – as expected – as a function of the solvent nature.

From cyclohexane to triethylamine, for a given solvent type, while $\mu(S_0)$ values appear to be slightly lower than those characterizing $\mu(S_1)$, the dipole moments $\mu(S_2)$ and $\mu(S_3)$ are largely decreased, by ~ 10 D, relative to the μ values in the two former states (GS and S_1) and almost coincide between themselves (with $\mu(S_3)$ being always of slightly smaller extent than $\mu(S_2)$). Within the same range of solvents, $\mu(S_4)$ has instead an intermediate value between these two extrema. Additionally, for the set of solvents with dielectric constant higher than in diethylamine, the dipole moment of BM decreases upon excitation towards S_1, the largest diminution – of at least ~ 10 D –

being observed for water, and N-Methylformamide. Accordingly, by considering these results BM tends to exhibit a larger dipole moment in the GS than that in S_1 for such solvents – and the reverse up to triethylamine – which is consistent with the experimental observations (see *e.g.* [75]). Such trend is indeed in quite good agreement with the supposed inverted solvatochromism if one calls to the commonly used features enabling a classification (*i.e.* change from positive to negative solvatochromism with increasing solvent polarity), suggesting that: $\mu(S_0)<\mu(S_1)$ in nonpolar solvents and reversibly $\mu(S_1)<\mu(S_0)$ in polar solvents for the transition $S_1 \leftarrow S_0$ [75] although some mystery still remains in this area from the experimental point of view, notably in link with the poor solubility of BM in apolar solvents, as stated previously. By making the very crude approximation of a perfect solubility of BM in apolar solvents and by using the TD-DFT CAM-B3LYP approach, one thus roughly recovers nevertheless the expected trend. However, according to these first observations and if one refers to the simple valence bond (VB) model [34,35], the point of reversal behavior seems to be slightly shifted nearer from diethylamine rather than being related to the expected chloroform solvent, usually proposed according to experimental results. Indeed, if this VB formalism is adopted, when each of the two N and S forms are characterized by equivalent (50%) contributions for the GS and the S_1 state, the cyanine-like limit (CL) for BM should be reached, involving that the dipole moment of both GS and S_1 is expected to be identical, with a zero change upon excitation. The firm conclusion among different experimental interpretations likely to account for reversal solvatochromism for this compound is beyond the scope of the present investigation. In particular, the potential involvement of self-aggregation phenomena supposed to hinder the assignment of wavelength shifts may also prevent from correct interpretation of solvatochromic aspects.

Apart from these phenomenological trends, it is important to get a more quantified overview of the lowest/highest charge separations. By comparing the whole set of dipole moment values (Table SI-2), the following conclusions can be drawn: (i) among all cases, the lowest values (with μ<10 D) are observed for S_2/S_3 in cyclohexane (9.6/9.2 D), carbon tetrachloride (9.8/9.5 D), benzene (9.9/9.5 D) and triethylamine (10.0/9.6 D); (ii) the highest value for each column (*i.e.* per kind of state) respectively corresponds to the case of BM considered with two explicit N-Methylformamide molecules for both GS (37.0 D), S_1 (24.0 D), and S_2 (23.3 D) while for S_3/S_4 it arises in the case of BM with two neighboring water molecules (20.3 D) (iii) except for solvents with dielectric constant (ε) lower than 4.24, the highest value among all states is almost systematically reached for S_4, the only exceptions to this trend observed for ε > 4.24 corresponding to water and N-Methylformamide in explicit solvent model, which on the reverse exhibit highest amounts of dipole moment for S_0 (35.8 D<μ<37.0 D); on the other hand, for apolar solvents, the highest μ value is instead observed either for GS or S_1 (19.8 D<μ<26.6 D). As a whole, these first observations constitute the premises allowing to expect ICT features distinction according to both

the excitation state/solvation medium kinds. According to ICT modulation, the considered transitions may be of interest compared to the bright ($S_1 \leftarrow S_0$) one, (despite oscillator strength values much lower for $S_n \leftarrow S_0$ transition (with n = 2, 3, 4, see Table SI-1).

2. Correlative ICT features

By focusing now on correlative ICT features, which can be estimated thanks to the Figure 3 and Table SI-3, few main trends are straightforward to identify. In SMD models, the minimal/maximal magnitudes of transferred charge ($|q_{CT}|$) are equal to [0.37/0.65] and [0.35/0.63], respectively, for the $S_1 \leftarrow S_0$ and $S_4 \leftarrow S_0$ transitions while as a whole for the $S_2 \leftarrow S_0$ and $S_3 \leftarrow S_0$ ones these extents are much higher, with [0.86/1.01] and [0.81/0.95] values, respectively. For calculations implying two explicit solvent molecules (in addition to the SMD treatment), *i.e.* BM+ES_2, these extrema values are generally slightly increased compared to the previous set, with for instance ranges equal to [0.41/0.70], and [0.39-0.58] for the $S_1 \leftarrow S_0$ and $S_4 \leftarrow S_0$ transitions, respectively. The same phenomenon arises for $S_2 \leftarrow S_0$ and $S_3 \leftarrow S_0$ transitions in such explicit conditions with [0.91/1.02] and [0.86/1.03] ranges, respectively. From these first observations, it appears that as a whole, one can anticipate ICT to be significantly influenced by the solvent along with a clear differentiation between the bright $S_1 \leftarrow S_0$ and the $S_2 \leftarrow S_0$ or $S_3 \leftarrow S_0$ transitions in terms of extent of charge flow, the $S_4 \leftarrow S_0$ one probably giving rise to the least interesting case (with even a lower $|q_{CT}|$ systematically observed for $S_4 \leftarrow S_0$ compared to $S_1 \leftarrow S_0$ except for apolar solvents below chloroform).

In line with the indications on $|q_{CT}|$ trends, the largest values of the charge-transfer dipole moment $|\Delta\mu_{CT}|$ are observed – and thus highest overall PET occurs – for the transitions towards ESs S_2 and S_3 (*i.e.* $S_2 \leftarrow S_0$ and $S_3 \leftarrow S_0$). This behavior holds true regardless the solvent type, although its nature plays a great role in the $|\boldsymbol{\mu}_{CT}|$ magnitude differentiation, with values around 10 D for apolar solvents and even as high as 20 D in the case of $S_3 \leftarrow S_0$ for water and N-Methylformamide environments. Reversely, the lowest $|\boldsymbol{\mu}_{CT}|$ systematically arises for $S_4 \leftarrow S_0$ transitions in almost all cases starting from the chloroform while these transitions are above the $S_1 \leftarrow S_0$ value by 4-5 D till triethylamine, and then just marginally increased by roughly ~1 D for diethylamine and diethylether. These evolutions on predicted q_{CT} and $|\boldsymbol{\mu}_{CT}|$ values are paralleled by the change in the D_{CT} extent, whose evolution as a function of solvent type has a large similitude with the $|\boldsymbol{\mu}_{CT}|$ trend. Nevertheless, it can be noticed that for water and N-Methylformamide, the differentiation in D_{CT} between S_2 and S_3 is almost inexistent. Nonetheless, the locations of the positive and negative displaced charge barycentres are dependent upon the

nature of S_n/solvation features and are either roughly localized as a whole on the bridge or on the bridge and more localized on the acceptor moiety, respectively.

3. ICT peculiarities in the light of chemical bonding/electron delocalization evolution

The trends of $|q_{CT}|$, D_{CT} and $|\boldsymbol{\mu}_{CT}|$ values – which were discussed in the previous section only in general terms – deserve to be analyzed in a more detailed manner, especially for a few specific cases in view of identifying their possible relationship with the evolution of chemical bonding and electron delocalization features upon vertical excitation. Apart from these PET global indices, which were collected for all systems and which will be examined hereafter according to various kinds of interest, the analyzed situations may also be distinguished in terms of the geometrical (HOMA) and electronic features (Δ_{FLU} and Δ_{DIcbcb}) listed in Table 1, which contains these data determined for a few case studies, as example of usefulness of such approach. The HOMA value is associated to the deviation of CC bond lengths in the 6CMR of the BM molecule from the value they have in the benzene molecule. Therefore, it provides a measure of the extent of bond length equalization in a ring, *i.e*. it corresponds to a sign of aromaticity. Based on its definition, HOMA equals one in benzene and becomes increasingly smaller than one with increasing bond length dissimilarity. Since vertical excitations are considered, the HOMA value for a given system remains fixed upon excitation. For instance, and as a first indication of usefulness of such data, it can be noticed that the HOMA values at GS clearly differentiate the media involving polar and (protic) polar solvents. While some earlier studies have depicted the Brooker's merocyanine as existing as a resonance hybrid which is weighted toward the zwitterion even in solvents of low dielectric constants [16] the actual situation is far from this view for this latter type of solvation. According to HOMA trends, the most representative form of BM in apolar/polar media at the GS shall rather correspond to polyene-like/zwitterion kinds. FLU is a measure of the deviation of the ring CC bond delocalization indices (DIs) from their single value in benzene. FLU is equal to zero in benzene and becomes larger than zero with decreasing perfect electron delocalization in the ring. FLU is here applied to the 6CMR of the BM molecule. DI_{cbcb} is instead the DI value of the central CC bond of CB of the BM molecule. For a single CC bond, DI is close to 1, depending on the wavefunction type and basis set and it reaches almost a value of 2 for a double CC bond. Δ_{FLU} and Δ_{DIcbcb} are the changes of FLU and DI_{cbcb} values, respectively, on passing from the GS to the vertical excited state *n*. Since GS frozen geometries are taken into account for ESs, these changes only reflect the electron density and exchange correlation density rearrangements upon excitation. They are generally dampened relative to those occurring in the corresponding adiabatic excitations where the nuclear positions rearrangement also plays a substantial role. Despite the clamped nuclei, we expect Δ_{FLU} to be negative (positive) if the CC bonds in the 6CMR become "electronically" more

(less) equalized upon excitation and Δ_{DIcbcb} to be positive (negative) if the central CC bond of the CB increases (decreases) its "electronic" double bond character upon excitation.

Beyond the above-mentioned delocalization indices along with ΔN(O) (*i.e.* the difference of the oxygen atom Bader's electron population N(O) on passing from the GS to the vertical excited state), Table 1 also provides the nature of centroid localization, C_{loc}, which denotes the location of the displaced charge centroids or barycenters of charge, $C_+(r)$ and $C_-(r)$. It has to be noted that these $C_+(r)/C_-(r)$, representing electron density increment/depletion barycenters, are most often displaced toward the donor (D)/the acceptor (A), respectively (*i.e.* Forwards-ICT, "F-ICT"). However, as a whole in the case of BM, these situations are not the prevalent ones, most of the charge transfers being instead of "Backwards-ICT" type with $C_+(r)$ and $C_-(r)$ being interverted compared to the conventional situation involving the electron transfer from the D to the A and thus leading to a negative $|\boldsymbol{\mu}_{CT}|$ value. For the less dominant "F-ICT" situations, the location is specified through a capital bold **F** as initial within the labels indicated in Table 1. Apart the possible initial "**F**", the different labels used in Table 1 serve to differentiate between main features trends. They have the following meaning : i) CB_{cent}: the two centroids are located roughly symmetrical relative to the 4CM (four-carbon-membered bridge or more simply 'Carbon Bridge' (CB) center and not too far from it ; CB_{ext}: one centroid is located at one extremum and the other at the other extremum of the CB; ii) *6CMR*: both centroids are located within the 6CMR (six-Carbon membered ring); iii) *6CMRCB*: one centroid is located within the 6CMR and the other approximately at the center of the CB; iv) $6CMR_{ext}CB$: one centroid is located within the 6CMR and the other roughly at the extremum of the CB close to the 6CMR; v) *CBMePy* (where MePy stands for Methyl-Pyridine ring), *i.e.*: one centroid is located roughly at the CB center and the other within the MePy; vi) $CB_{ext}MePy$: one centroid is located at the extremum of the CB close to the 6CMR and the other within the MePy.

The situations analyzed in detail in the next parts (3.1, 3.2, 3.3 and 3.4) have been clustered according to diverse kinds of interest (*i) The role of solvent modulation on ICT, ii) Strongly localized/delocalized ICT situations, iii) What brings to excitations with very high ICT features, iv) The situations leading to "Forwards-ICT")*. More precisely, a first category was selected to highlight either implicit or SMD+explicit ICT modulation induced through solvent effects by involving – in this latter case – solvent molecules interacting specifically with BM. A second kind of gathered cases is intended to characterize and contrast the local *vs* the CT nature of the excitation. Finally, a third one is selected to unveil features causing the highest $|\boldsymbol{\mu}_{CT}|$values for a given $S_n \leftarrow S_0$ (n = 1,4) excitation. Besides these three, a fourth category addresses the usual situation of CT from D to A (labelled "Forward-ICT" ("F-ICT")), *i.e.* situations in which electronic charge is transferred from the D to the A moiety of the BM molecule.

In order to intuitively observe the CT process under photo-excitation, the three PET global indices mentioned above (the D_{CT} and $|q_{CT}|$ values, along with the associated dipole moment variation) for all cases listed in Table 1 were graphically represented in Figures 4a-c and SI-2, in view of analyzing jointly the chemical bonding/electron delocalization evolution. In these Figures and superimposed on each molecular drawing is also shown i) the location of the transferred charge centroids represented through purple balls (*i.e.* $C_+(r)$ electron density increment barycenter/$C_-(r)$ electron density depletion barycenter). Additionally, Figures SI-3 and SI-4 represent the same kind of information in the case of the $S_1 \leftarrow S_0$ and the $S_4 \leftarrow S_0$ transitions, respectively, but extended here to the implicit solvation case for the whole range of solvents. Figure SI-5 provides an overview of the same features for the explicit treatment characterizing the BM+ES_2 systems of the $S_4 \leftarrow S_0$ transitions.

3.1The role of solvent modulation on ICT

As general trends, for the $S_1 \leftarrow S_0$ transition (Figure SI-3), the four solvents with the lowest ε values (cyclohexane, carbon tetrachloride, benzene, and triethylamine) exhibit Forwards-ICT ("F-ICT") features (these latter being detailed in part 3.4), while the implicit treatment of all remaining solvation situations leads to a Backwards-ICT ("B-ICT") effect. It can be noticed that, even if the conventional location of $C_+(r)$ and $C_-(r)$ leading to the electron transfer from the D to the A is only observed for the four above-mentioned solvents, the diethylamine, diethylether and chloroform cases are characterized by $|q_{CT}|$ values, which are very near from those of such F-ICT situations and only slightly differentiated between themselves. Nonetheless, they already display larger amounts of $|\boldsymbol{\mu}_{CT}|$ and D_{CT}. Starting from pyridine, rising values of the three PET global indices are observed as a result of ε augmentation, in link with the B-ICT effect. The confinement of $C_+(r)$ and $C_-(r)$ on the central positioning within the CC chemical bond (each one being on one side of this latter) observed for the solvents of lowest ε values progressively tends to evolve towards other situations starting from a symmetrical distance from these locations. By focusing on the effect of explicit solvent addition to the SMD treatment, it clearly induces a magnifying effect by raising the extent of both $|q_{CT}|$, $|\boldsymbol{\mu}_{CT}|$ and D_{CT}. At variance with $S_1 \leftarrow S_0$, none of the $S_2 \leftarrow S_0$ and $S_3 \leftarrow S_0$ transitions generates a reversal phenomenon while such effect reappears in the case of the $S_4 \leftarrow S_0$ excitation. Nevertheless, in that case it happens exactly in the opposite sense compared to the $S_1 \leftarrow S_0$ one (this latter effect being described in detail in part 3.4). PET global indices reveal that much higher CT extents are observed as a whole whatever the solvent type for the $S_2 \leftarrow S_0$ and $S_3 \leftarrow S_0$ transitions (all being of B-ICT type).

For a deeper analysis supported by the accurate examination of chemical bonding features, four different BM solvation situations of $S_n \leftarrow S_0$ (n = 1,4) transitions are considered as

representative cases (Table 1, first sub-section) namely i) water as implicit SMD model (Figure 4a, left), ii) water (SMD model) by including furthermore two explicit water molecules in addition to implicit treatment ("BM+ES_2 in water", Figure 4a, right), iii) aprotic benzene in implicit SMD treatment (Figure 4b, left), protic benzaldehyde as implicit SMD model (Figure 4b, right). As a whole, the case of N-Methylformamide in both implicit/explicit models is very similar to the one of water (it will be described in more details in part 3.2).

By considering first the $S_1 \leftarrow S_0$ transition, the main reason for the much higher $|\boldsymbol{\mu}_{CT}|$ values in either implicit (SMD treatment alone, *i.e.* "water") or explicit water (*i.e.* "BM+ES_2 in water") situations is the much larger extent of D_{CT} rather than the slightly larger transferred charge compared to other cases. This is clearly revealed by the C_{loc} parameter. Indeed, for these systems, characterized by higher $|\boldsymbol{\mu}_{CT}|$ values, the centroids are at the extremes of the CB (*i.e.* one centroid is located at one extremum and the other at the other extremum of the CB, $C_{loc} = CB_{ext}$), (Figure 4a, left/right). Reversely, in the case of implicit benzaldehyde and benzene solvent and even more particularly in this latter case, the two centroids are located in the inner part of this bridge, *i.e.* they are located roughly in a symmetrical manner relative to the CB center and not too far from it ($C_{loc} = CB_{cent}$). Another peculiarity characterizes the solvation in the benzene medium, thus switching in fact the C_{loc} into **F**CB_{cent}, in link with the F-ICT process occurring in such case, (see further indications section 3.4).

The much larger $|\boldsymbol{\mu}_{CT}|$ values for implicit and explicit water for $S_1 \leftarrow S_0$ transitions are paralleled by a strong enhancement of CC bond dissimilarity in the 6CMR. It corresponds to positive and large Δ_{FLU} (Δ_{FLU}*10 = 0.044 and 0.051, respectively). This effect is logically accompanied by a concomitant significant decrease of the double bond character of the CC central bond of the CB, hence negative and large in magnitude Δ_{DIcbcb} (Δ_{DIcbcb}*10= -1.700 and -1.941, respectively). On the contrary, in the case of benzene and benzaldehyde solvents, Δ_{FLU} is even largely negative (Δ_{FLU}*10 = -0.135 and -0.043, respectively) and Δ_{DIcbcb} is either positive in benzene (Δ_{DIcbcb}*10 = 0.429) or negative (but much less than for implicit or explicit water cases) in benzaldehyde (Δ_{DIcbcb}*10 = -0.693). These results clearly indicate that the $S_1 \leftarrow S_0$ excitation in the implicit and explicit water solvents implies a significant "electronic" shift of the BM molecule towards its polyene-like form, with the explicit water solvent molecules strengthening this effect. In benzaldehyde, the shift is strongly dampened, relative to water, and in benzene the shift is even reversed, that is leading to a situation evolving towards the zwitterionic form. The different evolution of the BM molecule upon $S_1 \leftarrow S_0$ excitation, as a function of the solvent type, is furtherly corroborated by the ΔN(O) values. If these latter are negative (positive), the electron population of the oxygen atom has decreased (increased) upon excitation, the opposite being true for the oxygen net atomic charge [nuclear charge - N(O)]. Indeed, ΔN(O) is largely negative for implicit and explicit water (-0.087 and -0.108, respectively), much less negative for benzaldehyde (-0.038)

and almost zero for benzene. The decrease of the O electron population upon $S_1 \leftarrow S_0$ excitation perfectly fits with the increased weight of the BM polyene-like form in implicit and explicit water solvents, whereas its increase in the benzene solvent complies with the BM evolution towards its zwitterionic form (Figure 1). The HOMA values examined for the four solvent cases demonstrate that the $|\boldsymbol{\mu}_{CT}|$and D_{CT}values for the $S_1 \leftarrow S_0$ excitation are – very logically – larger in situations for which a stronger 6CMR bond length equalization in the GS is observed. In other words, the switch of the BM molecule towards its polyene-like form is more significant the larger is the departure from this form in the GS.

The solvent effect for the $S_2 \leftarrow S_0$ and $S_3 \leftarrow S_0$ excitations may be analyzed in a similar way as in the $S_1 \leftarrow S_0$ transition, although one has to notice that for these excitations - at variance with the $S_1 \leftarrow S_0$ case - the BM molecule in benzene behaves similarly to the three other solvent media presented in Table 1. The displaced charge, $|q_{CT}|$, and the charge separation length, D_{CT}, exhibit large values in all solvation media. Despite their roughly similar $|q_{CT}|$, $|\boldsymbol{\mu}_{CT}|$ and D_{CT} trends as a function of the solvent type, the $S_2 \leftarrow S_0$ and $S_3 \leftarrow S_0$ excitations significantly differ for the location of the centroids of the displaced charge (Figure 4a-b). For the $S_2 \leftarrow S_0$ excitation, it is mostly located in the 6CMR, with the positive pole being placed in the CB for the case of larger $|\boldsymbol{\mu}_{CT}|$ values, while for the $S_3 \leftarrow S_0$ transition, the negative pole is shifted to the CB and the positive pole reaches the MePy moiety (Figure 4a-b). However, it shall be outlined that in the case of explicit water solvent (Figure 4a right), the features of S_2 and S_3 are interchanged, relative to the implicit water solvent case and to the other analyzed cases in this paragraph. This interchange may easily happen since the two mentioned states are extremely close in energy and could even be considered in fact as almost degenerate in implicit SMD model (Table SI-1), the two explicit molecules of the BM+ES_2 in water system inducing indeed a slight degeneracy lifting of the initial almost identical energy situation for S_2 and S_3. The same phenomenon also arises for implicit and explicit N-Methylformamide solvent cases, as stated in the next paragraph. The different location of centroids has a clear impact on the electronic similarity of the 6CMR CC bonds. When both centroids are located within the 6CMR (*i.e.* C_{loc} = 6CMR)) or close to it (C_{loc} = $6CMR_{ext}CB$, *i.e.* one centroid being located within the 6CMR and the other roughly at the extremum of the CB close to the 6CMR), Δ_{FLU} rather than being positive as it was the case for the $S_1 \leftarrow S_0$ excitations with large $|\boldsymbol{\mu}_{CT}|$values, is now largely negative. Conversely, when the positive pole reaches the MePy moiety (*i.e.* when one centroid is located at the extremum of the CB close to the 6CMR and the other within the MePy: C_{loc} = CB_{ext}MePy), Δ_{FLU} is largely positive, denoting a decrease of bond length equalization in the 6CMR. The case of a central location of the centroids (*i.e.* one centroid being located within the 6CMR and the other approximately at the center of the CB: C_{loc} = 6CMRCB) just represents an intermediate situation and Δ_{FLU} is accordingly close to zero. In all cases, except for the $S_3 \leftarrow S_0$ excitation in benzene solvent, the central CC bond of the CB significantly decreases its double

bond character (Δ_{DIcbcb} being largely negative) and the oxygen atom becomes less negatively charged (ΔN(O) being negative and in some cases to a very large extent). The situation of the $S_3 \leftarrow S_0$ excitation in benzene is peculiar given that it is characterized by negative Δ_{FLU} despite the positive centroid pole extension in direction of the MePy. Furthermore Δ_{DIcbcb} is largely positive rather than negative as in all other $S_2 \leftarrow S_0$ and $S_3 \leftarrow S_0$ excitations. Overall, the detailed analysis of these two latter types of excitations demonstrates that the BM molecule may exploit different charge flow mechanisms to achieve significant $|\boldsymbol{\mu}_{CT}|$ values whereas not all of them imply a concomitant decrease of electronic bond equalization in the 6CMR/double bond character of the central CC bond of the bridge. However, the large decrease of the oxygen atom electron population and the general decrease of the double bond character of the central CC bond of the bridge are all in favor of an increase of the weight of the polyene-like form upon excitation, even if the associated electronic signatures characterizing the 6CMR are not evident or even contradictory in some cases. The $S_4 \leftarrow S_0$ excitation is clearly different from all other ones involving ESs of lower energy than S_4. As a whole, as already mentioned, it is characterized by much smaller $|\boldsymbol{\mu}_{CT}|$ and D_{CT} values than those involved in $S_2 \leftarrow S_0$ and $S_3 \leftarrow S_0$ transitions (Figure 3), the same holding true for $|q_{CT}|$ values as well. Compared to $S_1 \leftarrow S_0$, higher $|\boldsymbol{\mu}_{CT}|$ and D_{CT} values are in that case observed till the chloroform, which served as crossover, while the reverse trend occurs afterwards for solvents ranked after this one in Figure 3. As will be detailed in part 3.4, by focusing on the sense at which CT occurs (*i.e.* forwards/backwards), solvent effects are characterized by an "opposite" reversal with respect to the $S_1 \leftarrow S_0$ transition. Among solvation situations considered in Table 1 in view of examining solvent effects (first sub-section of this Table), a forwards charge displacement ("F-ICT") is noticed for the $S_4 \leftarrow S_0$ transition in both benzaldehyde and implicit water as indicated through positive $\boldsymbol{\mu}_{CT}$. The common features for the $S_4 \leftarrow S_0$ transition are the occurrence of a very small positive or even negative Δ_{FLU} combined with a negative small or even positive Δ_{DIbcb} value, all factors leading, when properly associated, to the origin of the dampening effect of the CT process in this kind of excitation. While for $S_1 \leftarrow S_0$ transitions, the explicit treatment of solvation compared to the implicit one systematically raises the $|\boldsymbol{\mu}_{CT}|$ values of all solvation cases, the trend observed for $S_4 \leftarrow S_0$ ones is rather different, involving both situations in which it is augmented (chloroform, diethylamine and acetonitrile) or diminished (water and N-methylformamide). The only cases for which the $+ES_2$ model switches the direction of CT is the one of $S_4 \leftarrow S_0$ in water and in N-methylformamide, which both become B-ICT simply by adding the two explicit solvent molecules (such switching of sign of $\boldsymbol{\mu}_{CT}$ being never observed in the case of $S_1 \leftarrow S_0$ transitions for none of the solvents considered in the overall set of solvation media). These aspects therefore highlight the role played by specific interactions, which may differ from one excited state to the other.

3.2 Strongly localized/delocalized ICT situations

Concerning the second kind of selected examples presented in Table 1 in link with its "*Locally excited (LE) vs. charge transfer (CT) transitions*" sub-section, it can first be noted that the BM $S_1 \leftarrow S_0$ excitations in the triethylamine and diethylether solvents represent two cases of strongly localized excitation and extremely small $|\boldsymbol{\mu}_{CT}|$ value (Figure 4a, left and Table 1). Compared with the BM $S_3 \leftarrow S_0$ excitation in the implicit or explicit water solvation situation (Figure 4a, right), the $S_1 \leftarrow S_0$ excitations in the triethylamine and diethylether exhibit a $|\boldsymbol{\mu}_{CT}|$ value which is one order of magnitude smaller, essentially due to a quite smaller D_{CT} value. The transferred charge $|q_{CT}|$ is also smaller, but definitely not as much as the D_{CT} value, therefore leading to the strongly local character of these excitations (Figure 4b). The centroids of the displaced charge are both located close to the midpoint of the central CC bond of the CB and, solely in the case of triethylamine solvent, with a Forward polarity, or "Forwards-ICT" (F-ICT) (*i.e.* C_{loc} = FCB_{cent}). The BM $S_2 \leftarrow S_0$ excitation in cyclohexane represents an intermediate configuration, with a comparable $|q_{CT}|$ relative to the $S_3 \leftarrow S_0$ excitation in the implicit water solvent and a halved D_{CT} value, thus leading to a half large $|\boldsymbol{\mu}_{CT}|$ value. Its centroids of displaced charge are both located within the 6CMR (C_{loc} = 6CMR), while for the $S_3 \leftarrow S_0$ excitation in the implicit water model they lie twice as more apart one from the other, one at the extreme of the CB close to the 6CMR and the other within the MePy moiety (C_{loc} = CB_{ext}MePy). The very localized excitations, having quite small $|\boldsymbol{\mu}_{CT}|$ value, are characterized by the following trends: i) a significant increase rather than a decrease of electronic bond equalization in the 6CMR (with large and negative Δ_{FLU} values), ii) an almost negligible change of the oxygen net atomic charge and iii) the central CC bond of the CB acquiring significantly more double bond character (triethylamine) or being hardly perturbed (diethylether) upon excitation. Based on these data, and more specifically in the case of triethylamine solvent, the excitation appears to shift the BM molecule towards its polymethine-like and zwitterionic forms, though the charge centroids are in both solvents definitely far from being located at the extremes of the BM molecule (in fact the N atom of the MePy becomes imperceptibly less negatively charged in both solvents upon excitation). The series of $S_n \leftarrow S_0$ (n = 1-4) excitations in the implicit N-Methylformamide medium represents a situation in which the same solvent may lead to either LE or CT excitations, depending on which excited state is considered. While the first three excitations involve high $|\boldsymbol{\mu}_{CT}|$ values and a large separation of the extent of charge flow, with D_{CT} values as large as 3.5/4.2 Å, the $S_4 \leftarrow S_0$ excitation is definitely local in character, *i.e.* of LE type (D_{CT} = 0.9 Å) and has a very small and positive, rather than negative, $\boldsymbol{\mu}_{CT}$ value. This feature reveals a Forward polarity (*i.e.* "F-ICT") with the positive pole being located in the 6CMR (Figure SI-2, left). The $S_n \leftarrow S_0$ (n = 1-3) excitations are characterized by increasingly large D_{CT} values and different

locations of the displaced charge centroids, therefore highlighting different and increasingly more efficient ways to realize the separation of the poles of the transferred charge. Apart from the implicit solvent treatment, which is easily interpreted on the basis of what was already discussed above for other analyzed systems, it is noteworthy to outline the significant role played by explicit interactions of HB type between the polar (protic) solvent molecules and the acceptor moiety of BM on the localized/delocalized character of the CT excitations. For the $S_4 \leftarrow S_0$ excitation, as already outlined, this effect is clearly visible especially with respect to both the direction of the charge poles, which is reversed for the BM+ES_2 system in either explicit N-Methylformamide or water compared to the implicit solvent corresponding models (Figure SI-2 and Figure 4a, left *vs.* right, respectively). Furthermore, D_{CT} values are significantly larger in the explicit solvent situation. By gathering the C_{loc} information for $S_4 \leftarrow S_0$ on both kinds of solvents (Table 1 in the two first sub-sections), it is straightforward to identify a very similar behavior, with N-Methylformamide and water being both characterized by **F**6CMR$_{ext}$CB/6CMRCB in implicit/explicit treatments. In these situations, the explicit solvent molecules therefore act as a pivot element not only to invert the direction of charge flow but also to the switch from its more/less delocalized features.

3.3 What brings to excitations with very high ICT features

The third category of cases listed in the Table 1 (third-subsection) allows to analyze first the features leading to highest $|\boldsymbol{\mu}_{CT}|$ values for the various excitations in the implicit solvents. The $S_n \leftarrow S_0$ (n = 1-3) excitations with highest $|\boldsymbol{\mu}_{CT}|$ values are all those occurring either in water or in N-Methylformamide. When considering the case of SMD treatment, almost identical $|\boldsymbol{\mu}_{CT}|$ values are observed for $S_1 \leftarrow S_0$ and $S_3 \leftarrow S_0$ transitions in water and N-Methylformamide. The features within water medium are thus very much like those previously examined in detail for the corresponding excitations in the N-Methylformamide solvent, as already depicted. It is evident that the least efficient among the three excitations ($S_n \leftarrow S_0$ with n=1-3) in this solvation case - as far as the $|\boldsymbol{\mu}_{CT}|$ value is concerned - is the one where the charge displacement is confined within the CB ($S_1 \leftarrow S_0$, $|\boldsymbol{\mu}_{CT}|$ = -11.1 D). The efficiency increases when the positive pole displaces into the MePy moiety ($S_3 \leftarrow S_0$, $|\boldsymbol{\mu}_{CT}|$ = -18.7 D) and even more so when the negative pole moves inside the 6CMR one ($S_2 \leftarrow S_0$, $|\boldsymbol{\mu}_{CT}|$ = -19.3 D), with the remaining pole being still located within the CB in both cases. The two highest $|\boldsymbol{\mu}_{CT}|$ excitations are characterized by a very pronounced decrease of the double bond character of the CC central bond in the bridge and a noticeable decrease of the electron population of the oxygen atoms. When both decreases are particularly large, as it occurs for the $S_2 \leftarrow S_0$ excitation, the very high $|\boldsymbol{\mu}_{CT}|$ value is achieved even without reducing the CC bond electronic similarity in the 6CMR as testified by a Δ_{FLU} value being marginally different from zero.

The highest $|\boldsymbol{\mu}_{CT}|$ value for the $S_4 \leftarrow S_0$ excitation is found for the cyclohexane solvent. Differently from many $S_4 \leftarrow S_0$ transitions in other solvents (see part 3.4), it does not exhibit a forward charge displacement ("F-ICT") (Figure 4c), a situation usually implying a quite small $|\boldsymbol{\mu}_{CT}|$ value (see part 3.4). However, compared to the $S_n \leftarrow S_0$ (n = 1-3) transitions with highest $|\boldsymbol{\mu}_{CT}|$ values characterized by B-ICT and described above, its $|\boldsymbol{\mu}_{CT}|$ value is still relatively small (5.4 D). Indeed, both CC bond descriptors, *i.e.* Δ_{FLU} and Δ_{Dlcbcb}, as well as the increase of the O electron population, all comply with a shift of the BM molecule towards the zwitterionic form upon $S_4 \leftarrow S_0$ transition. It was already demonstrated that such kind of bonding evolution is not favorable for a high $|\boldsymbol{\mu}_{CT}|$ value.

Apart from the trend in SMD solvents, the cases of water or N-Methylformamide + ES_2 (explicit) treatment in $S_3 \leftarrow S_0$ transitions (mentioned in the previous sub-sections) lead to the enhancement of the effect already present in the corresponding SMD media.

3.4 The case of Forward-ICT ("F-ICT")

Revealing aspects observed in this case study with respect to F-ICT situations is of primarily importance for providing an overview of situations leading to this kind of charge flow, which is representative of what is commonly of high interest for applications. Furthermore, it is useful to provide a first clue towards a potential elucidation of the supposed reverse solvatochromism behavior of BM for the transition $S_1 \leftarrow S_0$ and for identifying conditions likely to lead to the occurrence of such ICT trend for transitions toward other ESs. Owing to the previously mentioned diethylamine case appearing - in the context of these TD-DFT calculations - as a pivot point for reversal of potential solvatochromic effects by using the conventional way of comparing the dipole moment between GS and S_0 state, the trends of SMD treatment for ε lower than the one exhibited by this solvent is of special interest. By focusing on these systems for $S_1 \leftarrow S_0$ (Figure SI-3), it appears that all expected cases (*i.e.* with ε below that of diethylamine: cyclohexane, carbon tetrachloride, benzene, and triethylamine) for which a F-ICT could be expected are indeed characterized by such effect (the other solvation cases being characterized by B-ICT). For all these four F-ICT situations, a C_{loc} of **F**CB_{cent} type is observed and the $|q_{CT}|$ amounts to +0.37 while $|\boldsymbol{\mu}_{CT}|$ and D_{CT} values lie in the ranges: 0.56 –0.91 D and 0.32–0.51 Å, respectively. For both $S_2 \leftarrow S_0$ and $S_3 \leftarrow S_0$ transitions, no cases of F-ICT are observed among the various SMD solvation treatments. Interestingly, for the $S_4 \leftarrow S_0$ transition (Figure SI-4), the B-ICT phenomenon now characterizes cyclohexane, carbon tetrachloride, benzene, triethylamine and diethylamine while a F-ICT occurs for all other solvent media considered in SMD treatment. The situation is thus inverted between

apolar/polar solvents in such case compared to the $S_1 \leftarrow S_0$ transition. Furthermore, both $|q_{CT}|$, $|\boldsymbol{\mu}_{CT}|$ and D_{CT} involved in these F-ICT transitions for the SMD model are as a whole of higher extent (0.44 < $|q_{CT}|$ < 0.60; 2.05 D < $|\boldsymbol{\mu}_{CT}|$ < 4.82 D; 0.82 Å < D_{CT} < 1.72 Å) than those observed for the $S_1 \leftarrow S_0$ transition (0.37 < $|q_{CT}|$ < 0.37; 0.56 D < $|\boldsymbol{\mu}_{CT}|$ < 0.91 D; 0.32 Å < D_{CT} < 0.51 Å). It is straightforward to observe within the $S_4 \leftarrow S_0$ excitations that a stronger evolution seems to take place from diethylether to N-Methylformamide than what was noticed between cyclohexane and triethylamine for $S_1 \leftarrow S_0$ ones. The C_{loc} are furthermore distinct, corresponding to FCB_{cent}/(F6CMRCB or F6CMR$_{ext}$CB) in the case of $S_1 \leftarrow S_0$/$S_4 \leftarrow S_0$ transitions. Additionally, while for the $S_1 \leftarrow S_0$ transitions, a marked difference exists between the two kinds of solvents in terms of these values, it is much less pronounced for the $S_4 \leftarrow S_0$ ones, since B-ICT solvents in that case (*i.e.* cyclohexane, carbon tetrachloride, benzene, triethylamine and diethylamine) are characterized as a whole – in SMD treatment – by: 0.35 < $|q_{CT}|$ < 0.63; 1.74 D < $|\boldsymbol{\mu}_{CT}|$ < 5.43 D; 1.03 Å < D_{CT} < 1.80 Å. Otherwise, adding explicit solvent molecules in the case of the F-ICT $S_4 \leftarrow S_0$ transitions induces a global lowering of all PET global indices for these situations (Figure SI-5).

As envisaged for other sections, a focus on more detailed information with respect to delocalization aspects of certain cases characterized by F-ICT may provide further insight. Concerning the selection of those situations reported in Table 1 (last sub-section) in view of studying them in detail, we can notice that they all imply very small and positive $\Delta\mu_{CT}$ values, as a result of small amounts of transferred charge and generally within a small distance in the BM molecule. All situations gathered in Table 1 for this sub-section are characterized by quite negative or marginally different from zero Δ_{FLU} and largely positive Δ_{DIcbcb} so that the electronic bond equalization in the 6CMR and the double bond character of the CC central bond in the CB is generally highly increased upon excitation, as expected in the case of a Forwards-ICT. This CC bond evolution agrees with a shift of the BM molecule towards the zwitterionic form for all these F-ICT transitions. Nevertheless, it can be noticed that for almost all F-ICT cases selected in Table 1, a decrease - rather than the expected increase - of the electron population of the oxygen atom may lead to a less simple interpretation, implying in fact an overall charge redistribution and some compensation effects. In these situations, the extent of global charge flow ($|q_{CT}|$) is anyway higher than the |ΔN(O)| and such phenomenon also occurs in fact for other situations linked to B-ICT instead of F-ICT. Otherwise, by looking at data gathered in the sub-section of Table 1 devoted to F-ICT examples in deeper detail, the higher extent of charge flow in the three specific cases (water, benzaldehyde and N-Methylformamide) considered for $S_4 \leftarrow S_0$ transitions with respect to the examples selected for the $S_1 \leftarrow S_0$ transition (*i.e.* benzene, triethylamine and cyclohexane) does not appear to be linked to expected chemical bonding features evolution. Indeed, when focusing on the ΔFLU*10 parameter, it can be noticed that this latter is very near from 0 for the three $S_4 \leftarrow S_0$ examined transitions while for the selected $S_1 \leftarrow S_0$ ones the expected negative ΔFLU*10 values

(owing to the F-ICT process) are observed. Δ_{Dlcbcb}*10 trends corroborate these aspects, being all positive and of higher absolute value in the case of $S_1 \leftarrow S_0$ excitations. The origin of such differentiation lies in the initial distinction of the weights of the different BM forms in GS, which is clearly stated through the GS HOMA amounts: between 0.388 and 0.638 for the first series ($S_4 \leftarrow S_0$ transitions) while it is noticeably diminished for the second one: ($S_1 \leftarrow S_0$ transitions) 0.122 and 0.145. Despite an initial (GS) situation with larger predominance of the zwitterionic form for the envisaged $S_4 \leftarrow S_0$ transitions, the polar solvents are prone to favor a very slight (further) CT effect. On the other hand, even if the 'starting' point in GS for the considered $S_1 \leftarrow S_0$ transitions seems to be much nearer to be a predominant polyene form, the apolar solvents have apparently (and logically) difficulties to induce a noticeable F-ICT.

4. Atomic groups decomposition of ICT

Thus far CT upon excitations were described in terms of cumulative values for the whole molecule (q_{CT}) and, in part 3.3, an analysis was provided in view of finding clues on how this global PET index correlates with the local evolution of bonding and electron delocalization. Although this already thorough analysis has provided chemically valuable information on the ICT process, further insight can be obtained by decomposing into atomic group contributions also all the global ICT indexes $|\boldsymbol{\mu}_{CT}|$, $|q_{CT}|$ and D_{CT}, thanks to the recently developed DOCTRINE code [45]. In the present investigation, a few representative cases with respect to the atomic group decomposition of the sole q_{CT} values were obtained by replacing the usual expression for q_{CT}, *i.e.* $q_{CT} = \int_{\text{all space}} \rho^{+}(\mathbf{r})\mathrm{d}\mathbf{r} \equiv \int_{\text{all space}} \rho^{-}(\mathbf{r})\mathrm{d}\mathbf{r}$, with $q_{\mathrm{CT}} = \sum_{\Omega} \int_{\Omega} \rho^{+}(\mathbf{r})\mathrm{d}\mathbf{r} \equiv \sum_{\Omega} \int_{\Omega} \rho^{-}(\mathbf{r})\mathrm{d}\mathbf{r}$ and where Ω are the atomic basins of the molecule defined through QTAIM [61]. While the integrals of ρ^{+} and ρ^{-} over all space or, analogously, summed up over all atomic basins are necessarily equal, those on a given basin or a group of basins are generally different, hence $\Delta q_{\mathrm{CT}}(\Omega) = \int_{\Omega} [\rho^{+}(\mathbf{r}) - \rho^{-}(\mathbf{r})]\mathrm{d}\mathbf{r}$ will generally differ from zero. In Figures 5a-c and SI-6a-b the $\Delta q_{\mathrm{CT}}(\Omega)$ values, grouped and summed up over chemically meaningful BM moieties (*i.e.* carbonyl oxygen, C6MR + 4H, central bridge + 2H, methylpyridine + 4H), are shown for a few significant cases. In the following, $\Delta q_{\mathrm{CT}}^{+}$ corresponds to the sum of only those atomic group contributions (Δq_{CT}) that are positive (the corresponding sum for the negative atomic group contributions, *i.e.* $\Delta q_{\mathrm{CT}}^{-}$, being equal to -$\Delta q_{\mathrm{CT}}^{+}$). Note that by definition $\Delta q_{\mathrm{CT}}^{+}$ is always lower than q_{CT} unless all atomic group basins have only points where the electron density is increased or only points where it is decreased. Usually, each atomic basin is characterized by the presence of both kinds of points, hence $q_{\mathrm{CT}} > \Delta q_{\mathrm{CT}}^{+}$ (or equivalently $q_{\mathrm{CT}} > |\Delta q_{\mathrm{CT}}^{-}|$). In the representative situations, which are depicted hereafter, $\Delta q_{\mathrm{CT}}^{+}$ is typically half the q_{CT} value. In Ref. 45, examples of atomic group decompositions of both $q_{\mathrm{CT}}^{+} = \sum_{\Omega} \int_{\Omega} \rho^{+}(\mathbf{r})\mathrm{d}\mathbf{r}$ and $q_{\mathrm{CT}}^{-} = \sum_{\Omega} \int_{\Omega} \rho^{-}(\mathbf{r})\mathrm{d}\mathbf{r}$ are also reported for BM in a few solvent systems cases.

Note that while the q_{CT}^{+} (or q_{CT}^{-}) [45] group decomposition strictly requires the DOCTRINE code, the evaluation of the atomic contributions to $\Delta q_{\mathrm{CT}}^{+}$ and to $\Delta q_{\mathrm{CT}}^{-}$ may also be performed by integrating the Bader's atomic electron populations of the GS and of the various ESs and by then taking their difference.

By focusing first on the case of BM considered in water with two explicit water molecules (BM+ES_2 in water, Figure 5a) for which the highest $|\boldsymbol{\mu}_{CT}|$ value among all solvents has been observed for three transition cases ($S_1 \leftarrow S_0$, $S_2 \leftarrow S_0$, $S_3 \leftarrow S_0$), the partitioning of Δq_{CT} into the contributions due to the various moieties highlights some interesting aspects. In the transitions involving the first three ESs, as expected owing to the B-ICT process, the (D)/(A) moieties of the BM molecule become negatively/positively charged, with the carbonyl oxygen atom playing an increasing role with rising $\Delta \mathrm{q}_{\mathrm{CT}}^{-}$ and $|\boldsymbol{\mu}_{CT}|$ values. The latter behavior is clearly aligned with the ΔN(O) trend in most cases (Table 1). The CB moiety is either negligibly perturbed ($S_1 \leftarrow S_0$) or either belongs to the donor ($S_2 \leftarrow S_0$) or to the acceptor ($S_3 \leftarrow S_0$) part of the molecule and never plays the dominant role in determining $\Delta q_{\mathrm{CT}}^{+}$ or $\Delta q_{\mathrm{CT}}^{-}$. The previously discussed peculiarity of the fourth excitation (parts 3.3-3.4) is reflected in the 6CMR acting as an electron acceptor, rather than a donor and, therefore, with only the distant carbonyl oxygen and the central bridge playing the role of donors. Such a situation unavoidably complies with small $\Delta \mathrm{q}_{\mathrm{CT}}^{-}$ and $|\boldsymbol{\mu}_{CT}|$ values.

In order to highlight the specific role played by explicit solvent water molecules, it is interesting to compare Figure 5a with Figure 5b where the Δq_{CT} decomposition for BM in implicit water solvent is illustrated. By taking into account the fact that the features of $S_2 \leftarrow S_0$ and $S_3 \leftarrow S_0$ are roughly interchanged when comparing the two situations (water *vs.* BM+ES_2 in water) – the explicit solvent molecules causing an inversion of the energies of these two excitations relative to the case of the implicit solvent model – it is easy to conclude that the main effect of the explicit solvent molecules for the first three excitations is only of quantitative nature, with percentage Δq_{CT} decompositions being in general slightly affected. However, in accordance with the F-ICT nature of the fourth excitation in the implicit water solvent model, important differences may be spotted for such a specific case. In the absence of explicit water solvent molecules, the MePy moiety has a small negative ($\Delta q_{\mathrm{CT}}(\Omega)$ = -0.057), rather than the usual largely positive $\Delta q_{\mathrm{CT}}(\Omega)$ value, and so acts as a BM electron donor moiety as do the carbonyl oxygen and the CB moieties. Instead, the 6CMR behaves as an electron acceptor as when the explicit solvent is present, but with a roughly doubled strength. The case of BM in N-Methylformamide with two explicit N-Methylformamide molecules (Figure SI-6a) closely resembles that of BM in water with two explicit water molecules for all excitations.

As a further point of comparison, Figure 5c illustrates Δq_{CT} decomposition for BM in cyclohexane by considering the transitions involving the first four ESs. Each excitation has its own

peculiar $\Delta q_{\mathrm{CT}}^{+}$. While $S_1 \leftarrow S_0$ has negligible $\Delta q_{\mathrm{CT}}^{+}$ as a result of negligible local contributions to $\Delta q_{\mathrm{CT}}^{+}$, $S_n \leftarrow S_0$ (*n* = 2-4) have quite larger $\Delta q_{\mathrm{CT}}^{+}$ values, yet realized in three well distinct ways. The role of electron donor is played by either the carbonyl oxygen alone (*n* = 2) or solely the 6CMR (*n* = 4), or all the BM molecule moieties except the MePy moiety (*n* = 3). This approach highlights the fact that $S_2 \leftarrow S_0$ and $S_3 \leftarrow S_0$ transitions in this solvation medium are characterized by quite similar $|\boldsymbol{\mu}_{CT}|$ values (-9.3 and -9.7 D), but realized through a different $\Delta q_{\mathrm{CT}}^{+}$ and, even more so, different BM moieties contributions to $\Delta q_{\mathrm{CT}}^{+}$ and hence to $\Delta \mathrm{q}_{\mathrm{CT}}^{-}$ as well. Δq_{CT} decomposition for BM in triethylamine exhibits very similar features to those observed for BM in cyclohexane and is reported in the Figure SI-6b.

CONCLUSION

In summary, we investigated by means of DFT/TD-DFT calculations the spectral and CT features of a few low-lying singlet excited states (S_1-S_4) by modulating the nature of solvent type in a model D−π−A compound, the *trans* Brooker's merocyanine, which is very sensitive to solvation effects. The reversal solvatochromism characterizing the transition $S_1 \leftarrow S_0$ is clearly observed both thanks to PET global indices but also in a more detailed manner through delocalization indices along with ΔN(O) features and the nature of centroid localization, C_{loc}. The rising dipole moment at the GS within the set of solvents considered leads to a situation progressively evolving in direction to a resonance hybrid, which is more weighted toward the zwitterion form for polar/protic solvents. As a result, for this kind of solvation media, a Backwards-ICT takes place upon excitation, while a Forwards-ICT only takes place for few solvents of low dielectric constant.

This thorough study allowed to highlight a few indicative trends about the trans-BM compound, among which are enclosed the following ones:

i) Whatever the solvent type, the brightest transition ($S_1 \leftarrow S_0$) characterizing the trans-BM molecule does not induce the largest CT situation; the dominating excited states for reaching the largest amount of CT systematically correspond to S_2 and S_3, with the lowest differentiation between $S_1 \leftarrow S_0$ and $S_3 \leftarrow S_0$ being observed for water and N-Methylformamide solvents (the largest gain in $|\boldsymbol{\mu}_{CT}|$ when comparing $S_1 \leftarrow S_0$ and $S_2/S_3 \leftarrow S_0$ arising instead for weak polar nonhydroxyl solvents). While the $|\boldsymbol{\mu}_{CT}|$ values for the two excited states (S_2 and S_3) are almost identical up to the chloroform, they progressively differentiate from each other and reach the highest distinction more specifically in water and in N-Methylformamide, the S_3 state being the most interesting one among these two. As a whole, among all cases treated within this study, the most

optimal situation when searching for an ideal efficiency of CT arises for $S_3 \leftarrow S_0$ in water and in N-Methylformamide, with an effective transfer of one electron and concomitantly the largest observed D_{CT} and $|\boldsymbol{\mu}_{CT}|$. Nevertheless, with respect to the direction of electron flow, for both and $S_2/S_3 \leftarrow S_0$ in all solvation media and $S_0 \leftarrow S_1$ except in this latter case for the four more apolar solvents, the ICT is of backwards type.

ii) The transition $S_4 \leftarrow S_0$ is characterized by an exactly opposed behavior compared to the one of $S_1 \leftarrow S_0$, with polar/protic solvents allowing a Forwards-ICT process, with the excited states S_4 being of higher dipole moment than the GS (whereas apolar solvents lead instead to Backwards-ICT for this $S_4 \leftarrow S_0$ transition).

iii) The location of the displaced charge barycenters is noticeably affected by the excited state and solvent nature or even by the type of such treatment (implicit *vs.* explicit). By using various implicit models with adjustable dielectric constant value, it has been evidenced that it has a clear incidence on this aspect. For benzene, the situation evolves from CB_{cent} ($S_1 \leftarrow S_0$) to 6CMR ($S_2 \leftarrow S_0$), CBMePy ($S_3 \leftarrow S_0$), and 6CMRCB ($S_4 \leftarrow S_0$) while for water conditions the evolution starts from CB_{ext} ($S_1 \leftarrow S_0$) and then goes towards 6CMRCB ($S_2 \leftarrow S_0$), CB_{ext}MePy ($S_3 \leftarrow S_0$) and R6CMR$_{ext}$CB ($S_4 \leftarrow S_0$). Taking into account explicit solvent changes the deal anyway. In particular, for $S_0 \leftarrow S_2/S_3$ transitions in water or N-Methylformamide media, consideration of explicit solvent molecules may induce an interchanged energy ordering of the excited states S_2 and S_3, which are very close in energy or even almost degenerate in implicit SMD model. In other media, instead of such slight lifting of the degeneracy, the initial differentiation in energy between implicit data of S_2 and S_3 leads – through the switching towards an explicit solvent procedure – to a decrease of their distinction. The $S_2 \leftarrow S_0$ transition is found to be mostly located in the 6CMR for all explicit solvent cases, except for the water and N-Methylformamide, for which it is mostly arising on the CB, the positive and negative poles being located at its extrema, for both situations. In contrast, this BM+ES_2 situation leads to an opposite trend for the $S_3 \leftarrow S_0$ excitation with the $C_+(r)$ and $C_-(r)$ being located on the CB except for the water and N-Methylformamide cases for which their location evolves towards the 6CMR section. Although displaced on it and characterized by distinct D_{CT} values, the charge barycenters for the explicit S_0-S_1 transitions are all roughly maintained on the CB section.

iv) Very localized electron flow mechanism in BM, involving quite small $|\Delta\mu_{CT}|$ value, are generally linked to an excitation that tends to shift the BM molecule towards its polymethine-like electronic structure. BM molecule may exploit different routes towards the achievement of significant $|\boldsymbol{\mu}_{CT}|$ values, not all of them implying a concomitant decrease of equalization bond length features in the 6CMR and double bond character

of the central CC bond of the bridge but this trend being clearly one possibility. As a representative case, the highest $|\boldsymbol{\mu}_{CT}|$ characterizing the water+ES_2 system, observed for $S_3 \leftarrow S_0$, clearly leads to a transformation of the BM molecule towards its zwitterionic form (such trend being already observed in the implicit model for the same transition but being largely reinforced by the HB effect).

Globally, the insight provided on the ICT processes by the investigated PET global indices is not just corroborated, but even largely enhanced by relating these indexes to the local evolution of bonding and electron delocalization upon excitation. The advantage of this further step is that of providing chemically valuable information on the ICT process. Additionally, the few representative results gained by employing the atomic group decomposition of one of the global ICT indexes, q_{CT}, demonstrate the interest of this further tool towards the goal of decrypting the ICT phenomenon into a chemical language.

Conflicts of interest
There are no conflicts to declare.

Acknowledgements

The authors gratefully acknowledge the support provided by the HPC resources and allocations of computing time from GENCI (IDRIS) and the facilities of the 'Mésocentre de Calcul Informatique Aquitain' (MCIA) of the University of Bordeaux, Pau, and 'Pays de l'Adour'. C. F. and Y. D. gratefully acknowledge the CNRS for the financial support of this research project through the PEPS ENERGIE 'SMARTBAT' grant.

ASSOCIATED CONTENT

Supporting Information

The Supporting Information enclosing complete description of computational details along with supplementary Tables and Figures is available free of charge via the Internet at http://pubs.acs.org.

AUTHOR INFORMATION

Corresponding Author
*E-mail: christine.frayret@u-picardie.fr

REFERENCES

(1) Juris, A.; Balzani, V.; Barigelleti, F.; Belser, P.; Von Zelewsky, A. Ru(II) Polypyridine Complexes: Photophysics, Photochemistry, Eletrochemistry, and Chemiluminescence. *Coord. Chem. Rev.*, **1988**, *84*, 85.

(2) Le Bahers, T.; Pauporté, T.; Scalmani, G.; Adamo, C.; Ciofini, I. A TD-DFT investigation of ground and excited state properties in indoline dyes used for dye-sensitized solar cells. *Phys. Chem. Chem. Phys.*, **2009**, *11*, 11276.

(3) García, G.; Adamo, C.; Ciofini, I. Evaluating push–pull dye efficiency using TD-DFT and charge transfer indices. *Phys. Chem. Chem. Phys.,* **2013**, *15*, 20210.

(4) Lemaur, V.; Steel, M.; Beljonne, D.; Brédas, J.-L.; Cornil, J. Photoinduced Charge Generation and Recombination Dynamics in Model Donor/Acceptor Pairs for Organic Solar Cell Applications: A Full Quantum-Chemical Treatment. *J. Am. Chem. Soc.*, **2005**, *127*, 6077.

(5) Li, Y.; Sun, C.; Song, P.; Ma, F.; Kungwan, N.; Sun, M. Physical Insight on Mechanism of Photoinduced Charge Transfer in Multipolar Photoactive Molecule. *Scientific Reports*, **2018**, *8*:10089.

(6) Kim, B.G.; Chung, K.; Kim, J. Molecular Design Principle of All-organic Dyes for Dye-Sensitized Solar Cells. *Chem. Eur. J.*, **2013**, *19*, 5220.

(7) Reichardt, C. Solvatochromic dyes as solvent polarity indicators. *Chem. Rev.*, **1994**, *94*, 2319.

(8) Anthonov, V.S.; Hohla, K.L. Dye stability under excimer-laser pumping. *Applied Physics B*, **1983**, *B32*, 9.

(9) Speiser, S.; Shakkour, N. Photoquenching parameters for commonly used laser dyes. *Applied Physics B*, **1985**, *B38*, 191.

(10) De Silva, A.P.; Gunaratne, H.Q.N.; Gunnlaugsson, T.; Huxley, A.J.M.; McCoy, C.P.; Rademacher, J.T., Rice, T.E. Signaling recognition events with fluorescent sensors and switches. *Chemical Reviews*, **1997**, *97*, 1515.

(11) Rémond, M.; Hwang, J.; Kim, J.; Kim, S.; Kim, D.; Bucher, C.; Bretonnière, Y.; Andraud, C.; Kim, E. Push–Pull Dyes for Yellow to NIR Emitting Electrochemical Cells. *Adv. Funct. Mater.,* **2020**, *30*, 2004831.

(12) Ohmori, Y. Development of organic light-emitting diodes for electro-optical integrated devices, *Laser Photonics Rev.*, **2010**, *4*, 2, 300.

(13) Pascal, S.; Bellier, Q.; David, S.; Bouit, P.-A.; HuiChi, S.; Makarov, N.; Le Guennic, B.; Chibani, S.; Berginc, G.; Feneyrou, P.; Jacquemin, D.; Perry, J. W.; Maury, O.; Andraud, C. Unraveling the Two-Photon and Excited State Absorptions of Aza-BODIPY Dyes for Optical Power Limiting in the SWIR band. *J. Phys. Chem. C*, **2019**, *123* (38), 23661.

(14) Merritt, I. C. D.; Jacquemin, D.; Vacher, M. Attochemistry: Is Controlling Electrons the Future of Photochemistry? *J. Phys. Chem. Lett.,* **2021**, *12* (34), 8404.

(15) Brooker, L. G. S.; Keyes, G. H.; Heseltine, D. W. Color and Constitution. XI.[1] Anhydronium Bases of p-Hydroxystyryl Dyes as Solvent Polarity Indicators, *J. Am. Chem. Soc*. **1951**, *73*, 5350.

(16) Morley, J. O.; Morley, R. M.; Docherty, R.; Charlton, M. H. Fundamental Studies on Brooker's Merocyanine. *J. Am. Chem. Soc.*, **1997**, *119*, 10192.

(17) Brooker, L. G. S. Some recent developments in the chemistry of photographic sensitizing dyes, *Experientia* Suppl. **1955**, *2*, 229.

(18) Hao, M.; Chi, W.; Wang, C.; Xu, Z.; Li, Z.; Liu, X. Molecular Origins of Photoinduced Backward Intramolecular Charge Transfer *J. Phys. Chem. C*, **2020**, *124*, 16820.

(19) Kulinich, A. V.; Mikitenko, E. K.; Ishchenko, A. A. Scope of negative solvatochromism and solvatofluorochromism of merocyanines, *Phys. Chem. Chem. Phys.,* **2016**, *18*, 3444.

(20) Kajiwara, K.; Osaki, H.; Greßies, S.; Kuwata, K.; Kim, J.-H.; Gensch, T.; Sato, Y.; Glorius, F.; Yamaguchi, S.; Taki, M. A negative-solvatochromic fluorescent probe for visualizing intracellular distributions of fatty acid metabolites, *Nature Communications*, **2022**, *13*, 2533.

(21) Nandi, L. G.; Facin, F.; Marini, V. G.; Zimmermann, L. M.; Giusti, L. A.; Da Silva, R.; Caramori, G. F.; Machado, V. G. Nitro-Substituted 4-[(phenylmethylene)imino]phenolates: Solvatochromism and Their Use as Solvatochromic Switches and as Probes for the Investigation of Preferential Solvent in Solvent Mixtures *J. Org. Chem.*, **2012**, *77*, 10668.

(22) Stock, R. I.; Nandi, L. G.; Nicoleti, C. R.; Schramm, A. D. S.; Meller, S. L.; Heying, R. S.; Coimbra, D. F.; Andriani, K. F.; Caramori, G. F.; Bortoluzzi A. J.; Machado, V. G. Synthesis and Solvatochromism of Substituted 4-(Nitrostyryl)phenolate Dyes. *J. Org. Chem.*, **2015**, *80*, 7971.

(23) Stock, R. I.; Schramm, A. D. S.; Rezende, M. C.; Machado, V. G. Reverse solvatochromism in solvent binary mixtures: a case study using a 4-(nitrostyryl)phenolate as a probe. *Phys. Chem. Chem. Phys.*, **2016**, *18*, 20266.

(24) Catalán, J.; Mena, E.; Meutermans, W.; Elguero, J. Solvatochromism of a typical merocyanine: stilbazolium betaine and its 2,6-di-tert-butyl derivative. *J. Phys. Chem.*, **1992**, *96*, 3615.

(25) Catalán, J. Do stilbazolium betaine dyes exhibit inverted solvatochromism by changes in solvent dipolarity? *Dyes and Pigments*, **2012**, *95*, 180.

(26) Da Silva, L.; Machado, C.; Rezende, M. C. On the solvatochromic reversal of merocyanine dyes. Part 1. The UV–VIS spectroscopic behaviour of vinylogous γ-pyridones *J. Chem. Soc., Perkin Trans. 2,* **1995**, *3*, 483.

(27) Da Silva, D. C.; Ricken, I.; Do, M. A.; Silva, R.; Machado, V. G. *J. Phys. Org. Chem.*, **2002**, *15*, 420.

(28) Bevilaqua, T.; Da Silva, D. C.; Machado, V. G. Preferential solvation of Brooker's merocyanine in binary solvent mixtures composed of formamides and hydroxylic solvents. *Spectrochim. Acta*, *Part A*, **2004**, *60*, 951.

(29) Abdel-Halim, S. T.; Awad, M. K. Absorption, fluorescence, and semiempirical ASED-MO studies on a typical Brooker's merocyanine dye. *J. Mol. Struct.*, **2005**, *754*, 16.

(30) Marder, S.R.; Perry, J.W.; Tiemann, B.G.; German, C.B.; Gilmour, S.; Biddle S.L.; Bourhill G. Direct observation of reduced bond length alternation in donor/acceptor polyenes. *J Am Chem Soc.*, **1993**, *115*, 2524.

(31) Marder, S.R.; Gorman, C.B.; Tiemann, B.G.; Cheng, L-T. Stronger acceptors can diminish nonlinear optical response in simple donor-acceptor polyenes. *J. Am. Chem. Soc.* **1993**, *115*, 3006.

(32) Dähne, S.; Nolte, K.-D. Model Realization of the Ideal Polymethine State by Solvent-Induced Changes in the Electronic Structure of Polymethine Dyes. *Acta Chim. Acad. Sci. Hung.*, **1978**, *97*, 147.

(33) Dähne, S. Systematik und Begriffserweiterung der Polymethinfarbstoffe. *Z. Chem.*, **1965**, *5*, 441.; Dähne, S.; Leupold, D. Der Polymethinzustand, *Ber. Bunsenges. Phys. Chem.*, **1966**, *70*, 618.; Dähne, S.; Moldenhauer, F. Structural Principles of Unsaturated Organic Compounds: Evidence by Quantum Chemical Calculations. *Progr. Phys. Org. Chem.* **1985**, *15*, 1.

(34) Förster, T. Color and constitution of organic compounds from the point of view of modern physics theories. *Z. Elektrochem. Angew. Phys. Chem.*, **1939**, *45*, 548.

(35) Platt, J. R. Wavelength Formulas and Configuration Interaction in Brooker Dyes and Chain Molecules *J. Chem. Phys*., **1956**, 25, 80.

(36) Würthner, F.; Archetti, G.; Schmidt, R.; Kuball, H.-G. Solvent effect on color, band shape, and charge-density distribution for merocyanine dyes close to the cyanine limit. *Angew. Chem., Int. Ed.*, **2008**, *47*, 4529.

(37) Dähne, S.; Radeglia, R. Revision der Lewis-Calvin-Regel zur charakterisierung vinyloger. Polyen- und polymethinähnlicher verbindungen. *Tetrahedron*, **1971**, *27*, 3673.

(38) Mustroph, H.; Mistol, J.; Senns, B.; Keil, D.; Findeisen, M.; Hennig, L. Relationship between the Molecular Structure of Merocyanine Dyes and the Vibrational Fine Structure of Their Electronic Absorption Spectra. *Angew. Chem. Int. Ed.*, **2009**, *48*, 8773.

(39) Gieseking, R. L.; Risko, C.; Brédas, J.-L. Distinguishing the Effects of Bond-Length Alternation *versus* Bond-Order Alternation on the Nonlinear Optical Properties of π-Conjugated Chromophores, *J. Phys. Chem. Lett.* **2015** *6* (12), 2158.

(40) Rezende, M. C.; Aracena, A. A general framework for the solvatochromism of pyridinium phenolate betaine dyes, *Chem. Phys. Lett.,* **2013**, 558, 77–81;

(41) Rezende, M. C. A generalized reversal model for the solvatochromism of merocyanines. *J. Phys. Org. Chem.*, **2016**, *29*, 460.

(42) Rettig, W., Dekhtyar, M. L.; Tolmachev, A. I.; Kurdyukov, V. V. *Chem. Heterocycl. Compd.*, **2012**, *47*, 1244; Letrun, R.; Koch, M.; Dekhtyar, M. L.; Kurdyukov, V. V.; Tolmachev, A. I.; Rettig, W.; Vauthey, E. *J. Phys. Chem. A*., **2013**, *117*, 13112.

(43) Mera-Adasme, R.; Moraga, D.; Medina, R.; Domínguez, M. Mapping the solute–solvent interactions for the interpretation of the three types of solvatochromism exhibited by phenolate-based dyes. *J. Mol. Liquids*, **2022**, *359*, 119302.

(44) Le Bahers, T.; Adamo, C.; Ciofini, I. A Qualitative Index of Spatial Extend in Charge-Transfer Excitations. *J. Chem. Theory Comput.*, **2011**, *7*, 2498.

(45) Gatti, C.; Danten Y.; Frayret, C. Atomic Group Decomposition of Charge Transfer Excitation Global Indexes. *J. Phys. Chem. A.*, **2022**, *126*, 36, 6314.

(46) Gaussian 16, Revision C.01, Frisch, M. J.; Trucks, G. W.; Schlegel, H. B.; Scuseria, G. E.; Robb, M. A.; Cheeseman, J. R.; Scalmani, G.; Barone, V.; Petersson, G. A.; Nakatsuji, H.; Li, X.; Caricato, M.; Marenich, A. V.; Bloino, J.; Janesko, B. G.; Gomperts, R.; Mennucci, B.; Hratchian, H. P.; Ortiz, J. V.; Izmaylov, A. F.; Sonnenberg, J. L.; Williams-Young, D.; Ding, F.; Lipparini, F.; Egidi, F.; Goings, J.; Peng, B.; Petrone, A.; Henderson, T.; Ranasinghe, D.; Zakrzewski, V. G.; Gao, J.; Rega, N.; Zheng, G.; Liang, W.; Hada, M.; Ehara, M.; Toyota, K.; Fukuda, R.; Hasegawa, J.; Ishida, M.; Nakajima, T.; Honda, Y.; Kitao,

O.; Nakai, H.; Vreven, T.; Throssell, K.; Montgomery, J. A., Jr.; Peralta, J. E.; Ogliaro, F.; Bearpark, M. J.; Heyd, J. J.; Brothers, E. N.; Kudin, K. N.; Staroverov, V. N.; Keith, T. A.; Kobayashi, R.; Normand, J.; Raghavachari, K.; Rendell, A. P.; Burant, J. C.; Iyengar, S. S.; Tomasi, J.; Cossi, M.; Millam, J. M.; Klene, M.; Adamo, C.; Cammi, R.; Ochterski, J. W.; Martin, R. L.; Morokuma, K.; Farkas, O.; Foresman, J. B.; Fox, D. J. Gaussian, Inc., Wallingford CT, 2016.

(47) Yanai, T.; Tew, D.P.; Handy, N.C. A new hybrid exchange–correlation functional using the Coulomb-attenuating method (CAM-B3LYP). *Chem. Phys. Lett.*, **2004**, *393*, 51.

(48) Marenich, A. V.; Cramer, C. J.; Truhlar, D. G. Universal Solvation Model Based on Solute Electron Density and on a Continuum Model of the Solvent Defined by the Bulk Dielectric Constant and Atomic Surface Tensions. *J. Phys. Chem. B*, **2009**, *113*, 6378.

(49) Guido, C. A.; Knecht, S.; Kongsted, J.; Mennucci, B. Benchmarking Time-Dependent Density Functional Theory for Excited State Geometries of Organic Molecules in Gas-Phase and in Solution. *J. Chem. Theory Comput.*, **2013**, *9*, 5, 2209.

(50) Jacquemin, D.; Perpete, E. A.; Scuseria, G. E.; Ciofini, I.; Adamo C. TD-DFT Performance for the Visible Absorption Spectra of Organic Dyes: Conventional versus Long-Range Hybrids*. J. Chem. Theory Comput.*, **2008**, *4*, 123.

(51) Pastore, M.; Mosconi, E.; De Angelis, F.; Grätzel, M. A Computational Investigation of Organic Dyes for Dye-Sensitized Solar Cells: Benchmark, Strategies, and Open Issues. *J. Phys. Chem. C* **2010,** *114,* 7205.

(52) Demoulin, B.; El-Tahawy, M. M. T.; Nenov, A.; Garavelli, M.; Le Bahers, T. Intramolecular photo-induced charge transfer in visual retinal chromophore mimics: electron density-based indices at the TD-DFT and post-HF levels. *Theoretical Chemistry Accounts*, **2016**, *135*, 96.

(53) Rudberg, E.; Sałek, P.; Helgaker T.; Agren, H. Calculations of two-photon charge-transfer excitations using Coulomb-attenuated density-functional theory. *J. Chem. Phys.*, **2005**, *123*, 184108.

(54) Peach, M. J. G.; Benfield, P.; Helgaker T.; Tozer, D. J. Excitation energies in density functional theory: An evaluation and a diagnostic test. *J. Chem. Phys.*, **2008**, *128*, 044118.

(55) Caricato, M.; Trucks, G. W.; Frisch M. J.; Wiberg, K. B. Oscillator Strength: How Does TDDFT Compare to EOM-CCSD? *J. Chem. Theory Comput.*, **2011**, *7*, 456.

(56) List, N. H.; Olsen, J. M.; Rocha-Rinza, T.; Christiansen O.; Kongsted, J. Performance of popular XC-functionals for the description of excitation energies in GFP-like chromophore models. *Int. J. Quantum Chem.*, **2012**, *112*, 789.

(57) Hayes, K. L. E. M.; Choczynski, M.; Crisci, R. R.; Wong, C. Y.; Dragonette, J.; Deschner, J.; Cardenas, A. J. P. Brooker's merocyanine: Comparison of single crystal structures. *J. Mol. Struct.*, **2018**, *1161*, 194.

(58) De Ridder, D. K J. A.; Heijdenrijk, D.; Schenk*,* H. Dimerization of Merocyanine Dyes. Structural and Energetic Characterization of Dipolar Dye Aggregates and Implications for Nonlinear Optical Materials. *Acta Cryst.*, **1990**, *C46*, 2197.

(59) Handy, N. C. On the evaluation of analytic energy derivatives for correlated wave functions, *J. Chem. Phys.*, **1984**, *81*, 5031.

(60) Ronca, E.; Angeli, C.; Belpassi L.; De Angelis, F.; Tarantelli, F.; Pastore M. Density relaxation in time-dependent density functional theory: combining relaxed density natural orbitals and multireference perturbation theories for an improved description of excited states. *J Chem Theor. Comput*., **2014**, *10*, 4014.

(61) Bader, R. F. W. *Atoms in Molecules: A Quantum Theory, Clarendon Press*, Oxford, **1994**.

(62) Gatti, C. SF-ESI code, private communication.

(63) Jara-Cortés, J.; Guevara-Vela, J.-M.; Pendás, Á. M.; Hernández-Trujillo, J. Chemical bonding in excited states: Energy transfer and charge redistribution from a real space perspective., *J. Comput. Chem.* **2017**, *38*, 957.

(64) Jara-Cortés, J.; Rocha-Rinza, T.; Hernández-Trujillo, J. Electron density analysis of aromatic complexes in excited electronic states: The benzene and naphthalene excimers, *Comput. Theor. Chem*., **2015**, *1053*, 220.

(65) Estévez-Fregosoa, M.; Hernández-Trujillo, J. Electron delocalization and electron density of small polycyclic aromatic hydrocarbons in singlet excited states, *Phys. Chem. Chem. Phys.*, **2016**, *18*, 11792.

(66) Casals-Sainz, J. L.; Jara-Cortés, J.; Hernández-Trujillo, J.; Guevara-Vela, J. M.; Francisco, E.; Pendás, Á. M. Chemical bonding in excited states: Energy transfer and charge redistribution from a real space perspective. *Chem. Eur. J.* **2019**, *25*, 12169.

(67) Terrabuio, L. A.; Haiduke, R. L. A.; Matta, C. F. Difluorodiazirine (CF_2N_2): A comparative quantum mechanical study of the first triplet and first singlet excited states, *Chem. Phys. Lett.*, **2016**, *655–656*, 96.

(68) Terrabuio, L. A.; Da Silva, N-A.; Haiduke, R.L.A.; Matta, C. F. Real space atomic decomposition of fundamental properties of carbon monoxide in the ground and the two lowest lying excited electronic states, *Molecular Physics*, **2017**, *115*, 1955.

(69) Jara-Cortés, J.; Matta, C. F.; Hernández-Trujillo, J. A fast approximate extension of the interacting quantum atoms energy decomposition to excited states. *J. Comput. Chem*., **2022**, 43, 16, 1068.

(70) Wang, L.L.; Azizi, A.; Momen, R.; Xu, T.; Kirk, R. S.; Filatov, M.; Jenkins, S. Next-generation quantum theory of atoms in molecules for the S_1/S_0 conical intersections in dynamics trajectories of a light-driven rotary molecular motor. *Int. J. Quantum Chem*., **2020**, *120*, 26062.

(71) Wang, L.; Azizi, A.; Xu, T.; Filatov. M.; Kirk, S.R.; Paterson, M. J.; Jenkins, S. The role of the natural transition orbital density in the $S_0 \rightarrow S_1$ and $S_0 \rightarrow S_2$ transitions of fulvene with next generation QTAIM, *Chem. Phys. Lett.*, **2020**, *751*, 137556.

(72) Tognetti, V., Joubert, L. Unraveling charge transfer processes with the quantum theory of atoms-in-molecules. *Theor. Chem. Acc.,* **2016**, *135*, 124.

(73) Campioli, E.; Sanyal, S.; Marcelli, A.; Di Donato, M.; Blanchard-Desce, M.; Mongin, O.; Painelli, A.; Terenziani, F. Addressing Charge-Transfer and Locally-Excited States in a Twisted Biphenyl Push-Pull Chromophore. *Chem.Phys.Chem.*, **2019**, *20* (21), 2860.

(74) Olsen, S. Locally-Excited (LE) versus Charge-Transfer (CT) Excited State Competition in a Series of Para-Substituted Neutral Green Fluorescent Protein (GFP) Chromophore Models. *J. Phys. Chem. B*, **2015**, *119* (6), 2566.

(75) Botrel, A.; Le Beuze, A.; Jacques, P.; Straub, H. Solvatochromism of a typical merocyanine dye. A theoretical investigation through the CNDO/SCI method including solvation. *J. Chem. Soc., Faraday Trans. II*, **1984**, *80*, 1235.

Solvent	$S_n \leftarrow S_0$	μ_{CT}, **D**	$\lvert q_{CT}\rvert$, **e⁻**	D_{CT}, **Å**	**C_{loc}**[a]	**Δ_{FLU}*10**[b]	**HOMA**[c]	**Δ_{DIcbcb}*10**[d]	**ΔN(O)**[e]
Solvent effect									
Benzene	$S_1 \leftarrow S_0$	+0.664	0.371	0.373	**F**CB_{cent}	-0.135	0.145	+0.429	0.000
Benzaldehyde	$S_1 \leftarrow S_0$	-5.822	0.508	2.387	CB_{cent}	-0.043	0.388	-0.693	-0.038
Water	$S_1 \leftarrow S_0$	-11.080	0.653	3.531	CB_{ext}	+0.044	0.638	-1.700	-0.087
Water+ES_2	$S_1 \leftarrow S_0$	-12.958	0.700	3.854	CB_{ext}	+0.051	0.804	-1.941	-0.108
Benzene	$S_2 \leftarrow S_0$	-9.742	0.861	2.355	6CMR	-0.219	0.145	-0.111	-0.332
Benzaldehyde	$S_2 \leftarrow S_0$	-15.020	0.952	3.286	6CMR_{ext}CB	-0.115	0.388	-0.984	-0.386
Water	$S_2 \leftarrow S_0$	-19.259	1.007	3.980	6CMRCB	-0.001	0.638	-1.570	-0.474
Water+ES_2	$S_2 \leftarrow S_0$	-15.013	0.761	4.107	CB_{ext}MePy	+0.025	0.804	-0.674	-0.130
Benzene	$S_3 \leftarrow S_0$	-10.130	0.815	2.587	CBMePy	-0.009	0.145	+0.620	-0.054
Benzaldehyde	$S_3 \leftarrow S_0$	-16.667	0.929	3.733	CB_{ext}MePy	+0.058	0.388	-0.342	-0.089
Water	$S_3 \leftarrow S_0$	-18.716	0.939	4.150	CB_{ext}MePy	+0.080	0.638	-0.760	-0.119
Water+ES_2	$S_3 \leftarrow S_0$	-20.835	1.025	4.233	6CMRCB	+0.006	0.804	-1.701	-0.506
Benzene	$S_4 \leftarrow S_0$	-4.478	0.541	1.724	6CMRCB	-0.210	0.145	+0.061	+0.025
Benzaldehyde	$S_4 \leftarrow S_0$	+4.824	0.587	1.710	**F**6CMRCB	-0.073	0.388	+0.114	-0.085
Water	$S_4 \leftarrow S_0$	+2.045	0.519	0.820	**F**6CMR_{ext}CB	+0.001	0.638	-0.200	-0.107
Water+ES_2	$S_4 \leftarrow S_0$	-3.399	0.513	1.378	6CMRCB	+0.006	0.804	-0.425	-0.124
Locally excited (LE) vs. charge transfer (CT) transitions									
Triethylamine	$S_1 \leftarrow S_0$	+0.562	0.371	0.315	**F**CB_{cent}	-0.132	0.157	+0.410	-0.002
Diethylether	$S_1 \leftarrow S_0$	-1.333	0.391	0.710	CB_{cent}	-0.105	0.251	-0.099	-0.011
Cyclohexane	$S_2 \leftarrow S_0$	-9.330	0.855	2.272	6CMR	-0.228	0.122	-0.061	-0.328
Water	$S_3 \leftarrow S_0$	-18.716	0.939	4.150	CB_{ext}MePy	+0.080	0.638	-0.760	-0.119
N-Methylformamide	$S_1 \leftarrow S_0$	+11.060	0.654	3.521	CB_{ext}	-0.043	0.623	+1.678	+0.085
	$S_2 \leftarrow S_0$	-19.076	1.006	3.949	6CMRCB	+0.000	0.623	-1.536	-0.468
	$S_3 \leftarrow S_0$	-18.692	0.937	4.152	CB_{ext}MePy	+0.081	0.623	-0.750	-0.119
	$S_4 \leftarrow S_0$	+2.229	0.530	0.875	**F**6CMR_{ext}CB	-0.001	0.623	-0.136	-0.107
N-Methylformamide+ES_2	$S_1 \leftarrow S_0$	-13.060	0.700	3.86	CB_{ext}	+0.085	0.791	-2.293	-0.105
	$S_2 \leftarrow S_0$	-13.790	0.710	4.02	CB_{ext}MePy	+0.038	0.791	-0.815	-0.125
	$S_3 \leftarrow S_0$	-20.880	1.030	4.22	6CMRCB	+0.036	0.791	-0.915	-0.492
	$S_4 \leftarrow S_0$	-4.650	0.530	1.84	6CMRCB	+0.048	0.791	-1.897	-0.120
What characterizes the highest $\lvert\Delta\mu_{CT}\rvert$ values among the various excitations									
Water	$S_1 \leftarrow S_0$	-11.08	0.653	3.531	CB_{ext}	+0.044	0.638	-1.700	-0.087
Water	$S_2 \leftarrow S_0$	-19.259	1.007	3.980	6CMRCB	-0.001	0.638	-1.570	-0.474
Water	$S_3 \leftarrow S_0$	-18.716	0.939	4.150	CB_{ext}MePy	+0.080	0.638	-0.760	-0.119
Cyclohexane	$S_4 \leftarrow S_0$	-5.432	0.629	1.797	6CMRCB	-0.227	0.122	+0.164	+0.035
Forwards intramolecular charge transfer ("F-ICT")									
Benzene	$S_1 \leftarrow S_0$	+0.664	0.371	0.373	**F**CB_{cent}	-0.135	0.145	+0.429	0.000
Triethylamine	$S_1 \leftarrow S_0$	+0.562	0.371	0.315	**F**CB_{cent}	-0.132	0.157	+0.410	-0.002
Cyclohexane	$S_1 \leftarrow S_0$	+0.907	0.369	0.511	**F**CB_{cent}	-0.141	0.122	+0.472	+0.001
Water	$S_4 \leftarrow S_0$	+2.045	0.519	0.820	**F**6CMRCB	+0.001	0.638	+0.200	-0.107
Benzaldehyde	$S_4 \leftarrow S_0$	+4.824	0.587	1.710	**F**6CMR_{ext}CB	-0.073	0.388	+0.114	-0.085
N-Methylformamide	$S_4 \leftarrow S_0$	+2.229	0.530	0.875	**F**6CMR_{ext}CB	-0.001	0.623	-0.136	-0.107

Table 1: Quantification of the PET extent on the BM molecule upon vertical excitation type ($S_n \leftarrow S_0$) from ground state (GS) to the first fourth excited states S_1, S_2, S_3 and S_4. Estimated ICT parameters related to the $S_n \leftarrow S_0$ transition: the transition dipole moment ($\boldsymbol{\mu}_{CT}$, in Debye, D), the absolute value of CT, $|q_{CT}|$ in e^-, and the charge-transfer length (D_{CT} in Å) corresponding to the distance between the two CT barycenters, along with other indices: **C_{loc}[a)], Δ_{FLU}*10[b], HOMA[c], Δ_{DIcbcb}*10[d]** and **ΔN(O) [e)]** defined below.

a) C_{loc} denotes the location of the centroids of the displaced charge, $q^+(r)$ and $q^-(r)$ (see Figures 4 and SI-2). For F-ICT situations, $C_+(r)/C_-(r)$, representing electron density increment/depletion barycenters, are displaced toward the acceptor (A)/the donor (D), respectively, whereas reverse situations ("B-ICT", "Backwards-ICT") also occur for the BM compound, in a predominant way. For F-ICT, the label location has a capital bold **F** as initial to indicate the "F-ICT" ("Forwards-ICT") nature of the CT. Apart the possible initial "**F**", the different labels have the following meaning. CB_{cent}: the two centroids are located roughly in a symmetrical manner relative to the Carbon Bridge (CB) center and not too far from it ; CB_{ext}: one centroid is located at one extremum and the other at the other extremum of the CB; 6CMR: both centroids are located within the 6CMR; 6CMRCB: one centroid is located within the 6CMR and the other approximately in the center of the carbon bridge; 6CMRextCB, one centroid is located within the 6CMR and the other roughly at the extremum of the CB close to the 6CMR; CBMePy, one centroid is located roughly at the CB center and the other within the MethylPyridine ring (MePy); CBextMePy: one centroid is located at the extremum of the CB close to the 6CMR and the other within the MePy.

b) Δ_{FLU} is the difference in the 6CMR FLU value on passing from the GS to the vertical excited state (ES), upon the absorption process, *i.e.* the difference between the final (ES) and the initial (GS) state of this phenomenon: $FLU_{ES} - FLU_{GS}$.

c) HOMA refers to such value for the 6CMR in the GS. The corresponding excited states retain the same HOMA value, since they all refer to vertical excitations.

d) Δ_{DIcbcb} is the difference in the value of the delocalization index **DI** of the ***c***entral CC ***b***ond of the ***c***arbon ***b***ridge on passing from the GS to the vertical excited state (ES), upon the absorption process, *i.e.* the difference between the final (ES) and the initial (GS) state of this phenomenon: $DI_{ES} - DI_{GS}$. DI_{cbcb} is an electronic measure of the single/double bond character of the central bond. Δ_{DIcbcb} is positive (negative) when the double bond character of the central bond increases (decreases) upon excitation.

e) ΔN(O) is the difference of the oxygen atom Bader's electron population N(O) on passing from the GS to the vertical excited state (ES), upon the absorption process, *i.e.* the difference between the final (ES) and the initial (GS) state of this phenomenon: $N(O)_{ES} - N(O)_{GS}$. If positive (negative), the electron population of the oxygen atom has increased (decreased) upon excitation, the opposite being true for the oxygen net atomic charge.

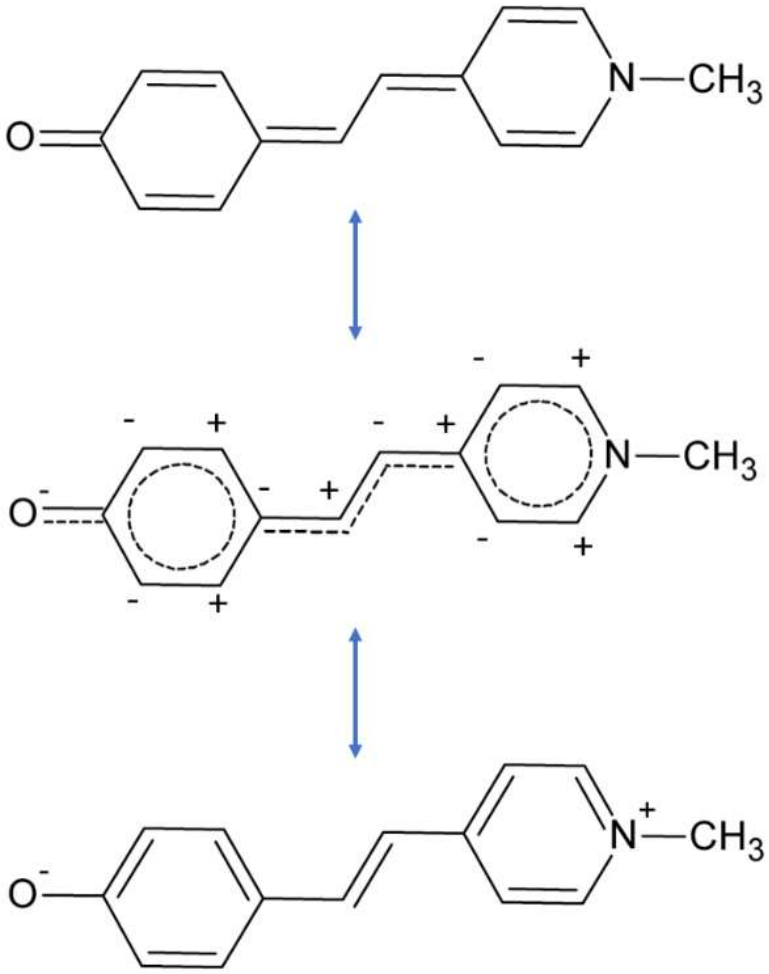

Figure 1: Brooker's merocyanine (BM): electronic structures change from polyene-like (bond-alternated) (top) via equilibrated (non-alternated) polymethine-like, $(BM)_{pm}$ (middle) to fully reversed (bond-alternated) zwitterionic state, $(BM)_b$ (bottom) states.

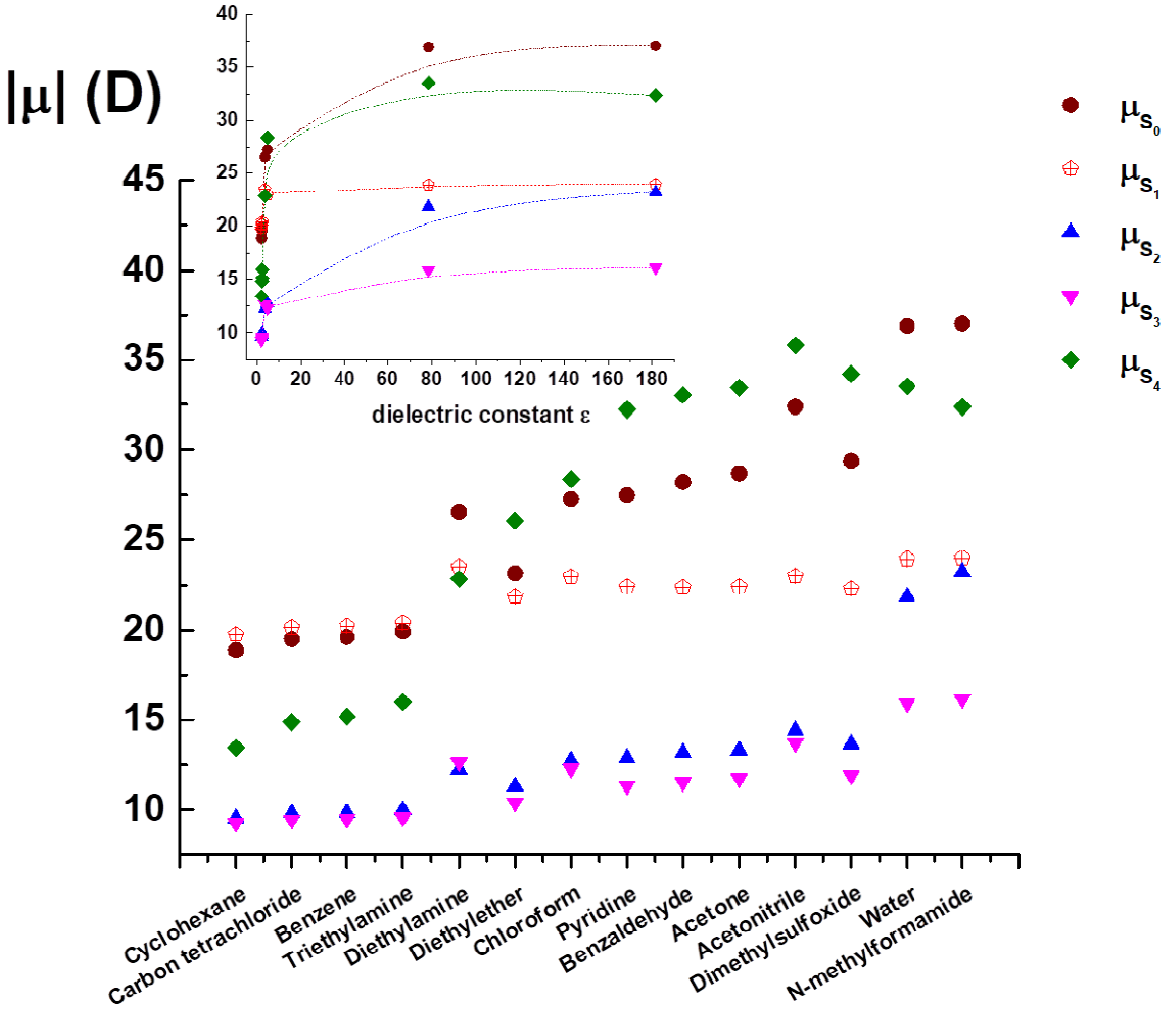

Figure 2: Representation of the dipole moment values |μ| as a function of solvent nature for the S_0 (GS) and S_1, S_2, S_3, S_4 vertical excited states. The smallest graph – presented as an insert of the major one – corresponds to an alternative representation as a function of the dielectric constant of solvents. For the set of following solvents: acetonitrile, diethylamine, chloroform, water and N-Methylformamide, the values correspond to the cases involving two explicit solvent molecules in addition to the SMD model (*i.e.* system BM+ES_2).

a)

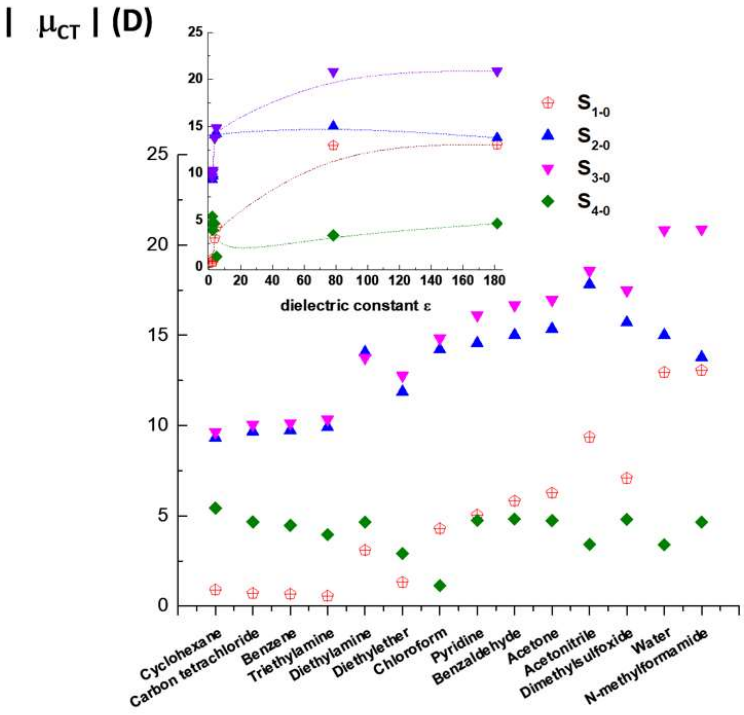

b)

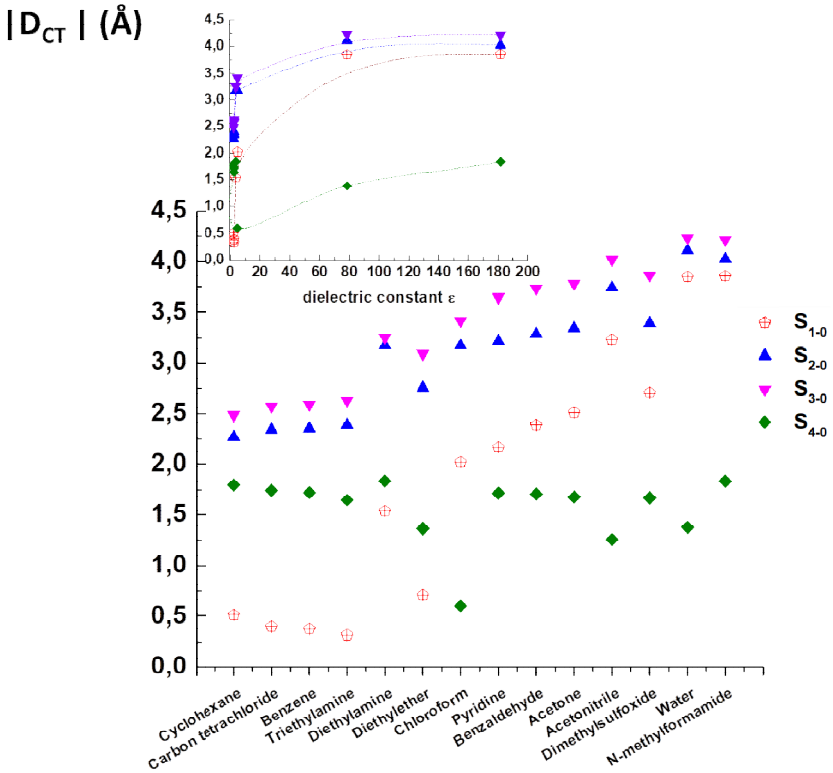

Figure 3: a) Representation of the transition dipole moment values $|\boldsymbol{\mu}_{CT}|$ for the $S_n \leftarrow S_0$ (n = 1-4) transitions as a function of solvent nature. The smallest graph – presented as an insert of the major one – corresponds to an alternative representation as a function of the dielectric constant of solvents. For the set of following solvents: acetonitrile, diethylamine, chloroform, water and N-Methylformamide, the values correspond to the cases involving two explicit solvent molecules in addition to the SMD model (*i.e.* system BM+ES_2). b) Representation of the charge-transfer length (D_{CT}) (*i.e.* distance between the two ICT barycenters) as a function of solvent nature for the $S_n \leftarrow S_0$ (n = 1-4) transitions. The smallest graph – presented as an insert of the major one – corresponds to an alternative representation as a function of the dielectric constant of solvents. For the set of following solvents: acetonitrile, diethylamine, chloroform, water and N-Methylformamide, the values correspond to the cases involving two explicit solvent molecules in addition to the SMD model (*i.e.* system BM+ES_2).

a)

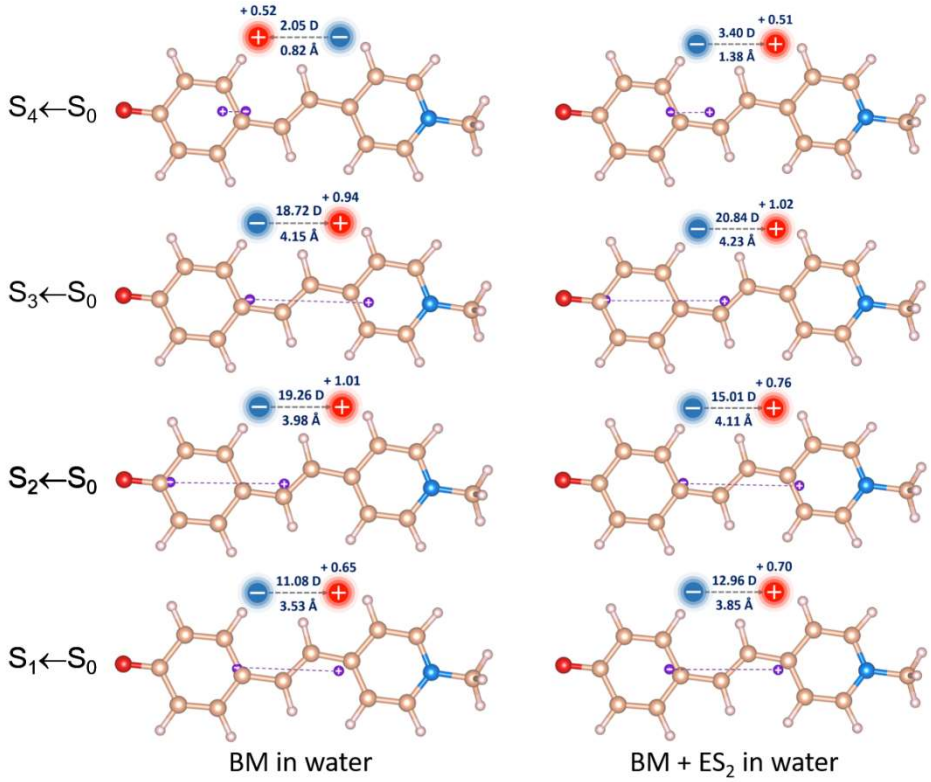
S4←S0
S3←S0
S2←S0
S1←S0
+0.52
2.05 D
0.82 Å
+0.51
3.40 D
1.38 Å
+0.94
18.72 D
4.15 Å
+1.02
20.84 D
4.23 Å
+1.01
19.26 D
3.98 Å
+0.76
15.01 D
4.11 Å
+0.65
11.08 D
3.53 Å
+0.70
12.96 D
3.85 Å
BM in water
BM + ES2 in water

b)

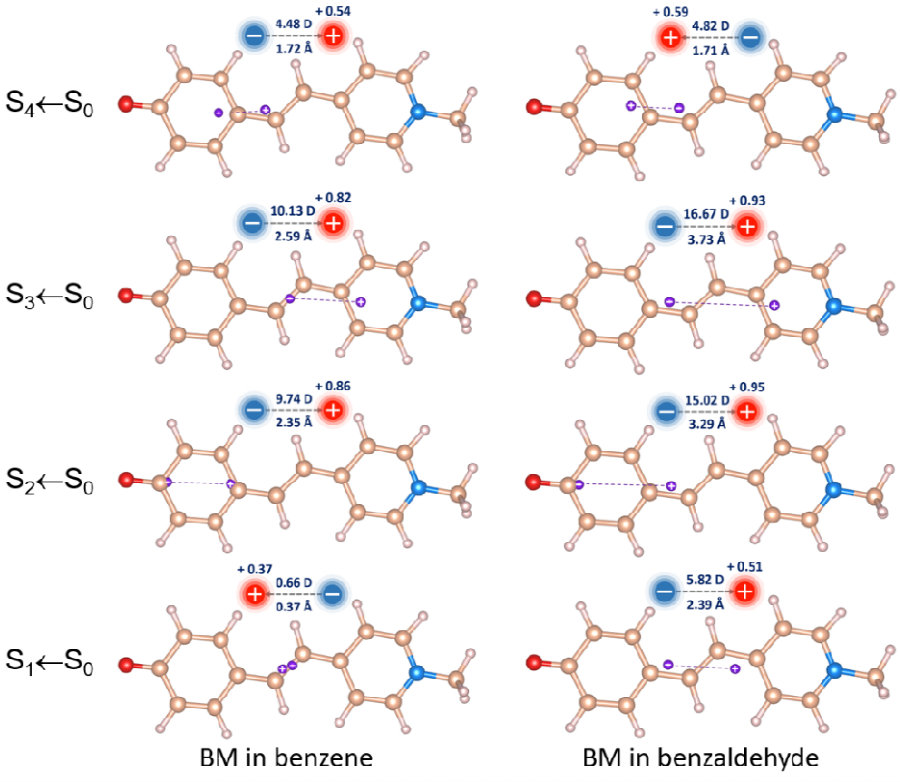
S4←S0
S3←S0
S2←S0
S1←S0
+0.54
4.48 D
1.72 Å
+0.59
4.82 D
1.71 Å
+0.82
10.13 D
2.59 Å
+0.93
16.67 D
3.73 Å
+0.86
9.74 D
2.35 Å
+0.95
15.02 D
3.29 Å
+0.37
0.66 D
0.37 Å
+0.51
5.82 D
2.39 Å
BM in benzene
BM in benzaldehyde

c)

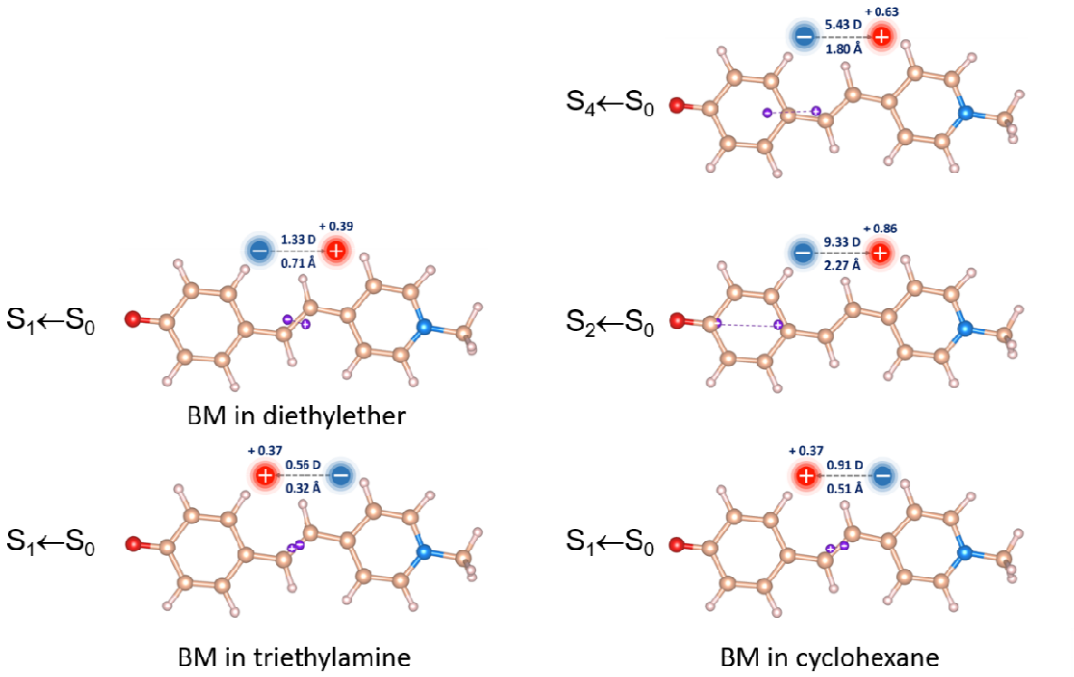

Figure 4: Representation of ICT parameters: $|\boldsymbol{\mu}_{CT}|$, the transition dipole moment values in Debye (D), the transferred charge $|q_{CT}|$ and D_{CT}, the charge-transfer length in Å of the BM molecule for the S_n←S_0 transitions in different solvents, according to the four PET categories displayed in Table 1 in which the location of the centroids of transferred charge (positive and negative poles) is also indicated (purple balls *i.e.* C_+(r) electron density increment barycenter/C_-(r) electron density depletion barycenter). The various graphs are plotted for the following situations: a) water using only an implicit SMD model (left) and by including also two explicit solvent molecules interacting with BM in addition to the SMD model (BM+ES_2, right); b) SMD model of benzene (left) and benzaldehyde (right); c) S_n←S_0 (n = 1) transition in SMD model of triethylamine and diethylether (left) and S_n←S_0 (n = 1, 2, 4) transitions in SMD model of cyclohexane (right).

a)

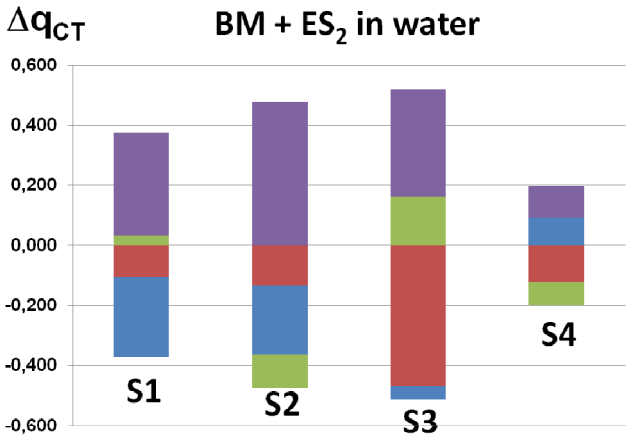

b)

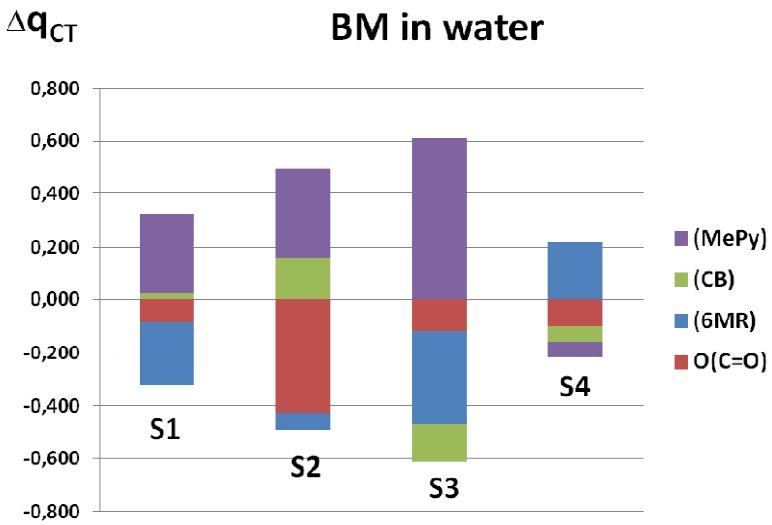

c)

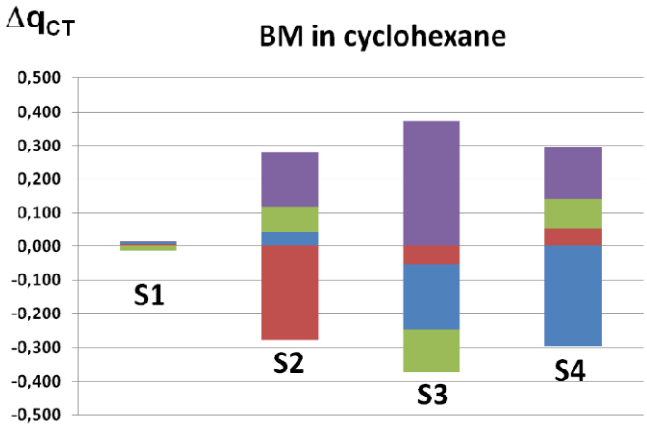

Figure 5: $\Delta q_{CT}(\Omega)$ values resulting from atomic group decomposition, grouped and summed up over chemically meaningful BM moieties (carbonyl oxygen, C6MR + 4H, central bridge + 2H, methylpyridine + 4H) for the CT process involving BM the following situations: a) in water when two explicit solvent molecules interact with C=O group of BM in addition to the SMD model: *i.e.* BM+ES_2) b) when only the implicit SMD water model is adopted and c) when cyclohexane in the implicit SMD model is considered.